



The tectono-stratigraphic architecture of the Falkland Plateau basin; implications for the evolution of the Falkland Islands Microplate



Roxana M. Stanca^{a,*}, Dave J. McCarthy^b, Douglas A. Paton^c, David M. Hodgson^a, Estelle J. Mortimer^a

^a School of Earth and Environment, University of Leeds, Leeds LS2 9JT, United Kingdom

^b Lyell Centre, British Geological Survey, Edinburgh EH14 4AP, United Kingdom

^c TectonKnow, Settle BD24 9FD, United Kingdom

ARTICLE INFO

Article history:

Received 27 November 2020

Revised 1 September 2021

Accepted 14 September 2021

Available online 5 October 2021

Handling Editor: N. Rawlinson

Keywords:

Seismic reflection

Microplate

Stress field

Extensional tectonics

South-western Gondwana

ABSTRACT

Commonly, intra-continental wrenching is associated with a high degree of crustal faulting and fragmentation. The resulting continental blocks can undergo vertical-axis rotations, which in turn can lead to the generation of intricate fault networks within and along their boundary regions. Investigations into these structural complexities can support understanding of when and how these continental blocks rotate, and what their position was prior to transform margin formation. In the case of the Falkland Islands Microplate (part of the Falkland Plateau transform margin), its position between South Africa, South America, and East Antarctica prior to the break-up of Gondwana is still debatable. This uncertainty affects the reliability of plate models for this region. Here we integrate gravity and 2D and 3D seismic reflection data from the eastern margin of the microplate (west side of the Falkland Plateau Basin) to provide insights into the tectono-stratigraphic architecture of this area from Jurassic onwards, and into the evolution of the Falkland Islands Microplate. Our findings show that the western part of the Falkland Plateau Basin is an integral part of the microplate, and it underwent deformation in a relatively fast-changing stress regime. Stress field configuration estimates across the Falkland Islands Microplate support an alternation between a NE-SW and NW-SE/WNW-ESE orientation of σ_3 during the Jurassic and an ENE-WSW oriented σ_3 during the Lower Cretaceous. Correlations of this local stress configuration with the regional support a Middle to Upper Jurassic rotation of the microplate in a predominantly extensional setting facilitated by the early fragmentation of south-western Gondwana.

© 2021 The Authors. Published by Elsevier B.V. on behalf of International Association for Gondwana Research. This is an open access article under the CC BY license (<http://creativecommons.org/licenses/by/4.0/>).

1. Introduction

Typically, intra-continental wrenching is associated with high degrees of crustal fragmentation and rotations of the resulting crustal and lithospheric blocks (Scrutton, 1979; Mascle et al., 1987; Nemčok et al., 2016; Ingersoll and Coffey, 2017). This leads to structurally complex isolated blocks where smaller, secondary fault systems within and along their boundaries accommodate relatively large rotations (Ron et al., 1984; McKenzie and Jackson, 1986; Peacock et al., 1998; Platt and Becker, 2013). The analysis of these fault networks can offer more insights into the temporal variation in the stress regime that affected the blocks, which can be used to aid reconstruction models. The Falkland Islands Microplate (FIM) is an example of an isolated block developed in an intra-continental wrenching setting. The FIM is part of the larger

Falkland Plateau transform margin that underwent intense deformation during the fragmentation of Gondwana and the opening of the South Atlantic in the Mesozoic due to wrenching between East and West Gondwana, and South America and Africa (Rabinowitz and Labrecque, 1979; Lorenzo and Mutter, 1988; Platt and Philip, 1995; Richards et al., 1996; Richards and Fannin, 1997; Bry et al., 2004; Del Ben and Mallard, 2004; König and Jokat, 2006; Kimbell and Richards, 2008; Baristead et al., 2013; Lohr and Underhill, 2015; Schimschal and Jokat, 2019). Although there are uncertainties in the nature of the FIM boundaries, we define and refer to this block as a microplate due to its scale and different motion during the fragmentation of Gondwana compared to the surrounding major tectonic plates.

Extensive work has been undertaken looking at the deformation affecting the FIM, which resulted in onshore to offshore fault network compilations and crustal architecture models (Ludwig et al., 1978; Lorenzo and Mutter, 1988; Platt and Philip, 1995; Richards et al., 1996; Richards and Fannin, 1997; Thomson, 1998; Curtis

* Corresponding author.

E-mail address: r.m.stanca@leeds.ac.uk (R.M. Stanca).

and Hyam, 1998; Aldiss and Edwards, 1999; Bry et al., 2004; Del Ben and Mallardi, 2004; Kimbell and Richards, 2008; Schreider et al., 2011; Baristead et al., 2013; Lohr and Underhill, 2015; Schimschal and Jokat, 2019). However, no detailed structural analysis has been published for the eastern boundary of the FIM (the western margin of the Falkland Plateau Basin). This scarcity of information hinders attempts to generate a reliable reconstruction model for the microplate and the entire plateau.

This study aims to document the western part of the Falkland Plateau Basin, and its constituent depocentres: the Volunteer and Fitzroy sub-basins. Their present-day tectono-stratigraphy reflects the complexities of transform margins and was in addition influenced by the development of the plateau between South America, Africa, and East Antarctica. This study focuses on the area that would have sat between the Falkland Islands and South Africa in a rotational reconstruction model (Adie, 1952; Mitchell et al., 1986; Marshall, 1994; Curtis and Hyam, 1998; Thomson, 1998; Trewin et al., 2002; Stanca et al., 2019) by assessing the fault network and stratigraphic architecture of this region. This facilitates the analysis of the nature of the deformation that occurs within and around the margins of a rotated microplate. Furthermore, the results are discussed in the context of south-western Gondwana by comparing the local and regional stress regimes.

2. Geological background

2.1. Overview of the Falkland Plateau

The Falkland Plateau (FP) is located east of Argentina, extending eastward ~2000 km away from the Argentinian coast. It is bounded to the north by the dextral Agulhas - Falkland Fracture Zone (AFFZ) and to the south by the North Scotia Ridge (NSR) (Ludwig, 1983; Richards et al., 1996) (Fig. 1). The formation of the FP was associated with the break-up of Gondwana and the opening of the Atlantic Ocean in the Mesozoic (Upper Triassic – Upper Cretaceous) and was subsequently affected by oblique compression and transpression related to sinistral strike-slip movement during the development of the NSR (Lorenzo and Mutter,

1988; Uliana et al., 1989; Cunningham et al., 1998; Eagles, 2000; Macdonald et al., 2003; Bry et al., 2004; Heine et al., 2013). The behaviour of the FP during the break-up remains controversial. Correlations between geological and geophysical data from the Falkland Islands and South Africa led to the development of the rotational theory which argues that the formation of the FP was accompanied by up to 120° rotation of the Falkland Islands (Adie, 1952; Mitchell et al., 1986; Marshall, 1994; Mussett and Taylor, 1994; Thomson, 1998; Curtis and Hyam, 1998; Storey et al., 1999; Trewin et al., 2002; Macdonald et al., 2003; Stone et al., 2009; Stanca et al., 2019). The lack of documented evidence for this rotation in the sedimentary infill of the basins surrounding the islands (Richards et al., 1996), and the absence of a mechanism to accommodate this rotation led several authors to favour a non-rotational model. In this model, the Falkland Islands were in a similar position relative to South America prior to the break-up of Gondwana as today (Lawrence et al., 1999; Ramos et al., 2017; Lovecchio et al., 2019; Eagles and Eisermann, 2020), and the fragmentation of the supercontinent was recorded by extension in the sedimentary basins around the islands.

Regardless of the movement of the Falkland Islands, the fragmentation of Gondwana and the initial rifting in the South Atlantic resulted in a series of structural and crustal provinces along the FP. These are, from west to east: the Malvinas Basin, the Falkland Islands (FI) with the North Falkland Basin to the north and the South Falkland Basin to the south, the Falkland Plateau Basin (FPB), and the Maurice Ewing Bank (Fig. 1). The North Falkland Basin is further subdivided in the Jurassic Southern North Falkland Basin (SNFB) and the Upper Jurassic-Lower Cretaceous North Falkland Graben (Lohr and Underhill, 2015; Stanca et al., 2019). The FPB consists of the Volunteer sub-basin to the north-west and the Fitzroy sub-basin in the west and south-west, the two being separated by the Berkeley Arch basement high (Rockhopper Exploration Plc., 2012; Dodd and McCarthy, 2016) (Fig. 1).

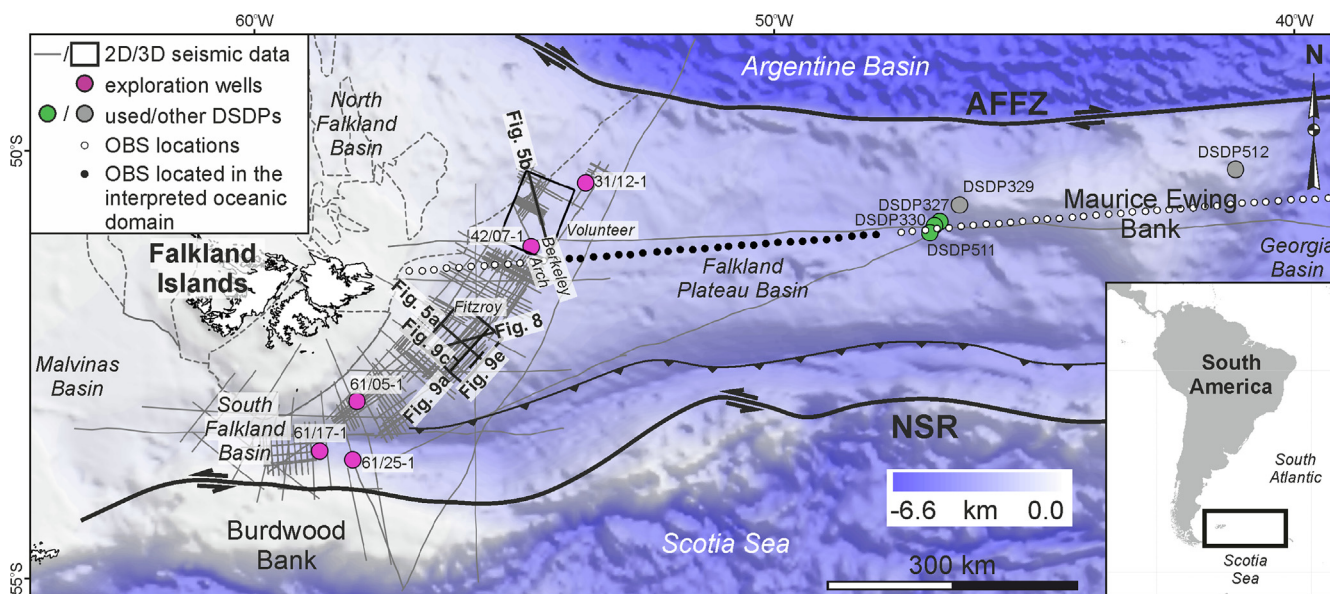


Fig. 1. Bathymetric map (GEBCO Compilation Group, 2020) of the Falkland Plateau (FP), overlain by the seismic reflection, exploration well, and Deep Sea Drilling Project (DSDP) data utilised in this study. The map shows the FP constituent basins (grey, dashed lines) and the regional structures bounding it (dextral and sinistral Agulhas - Falkland Fracture Zone and North Scotia Ridge, respectively, and the thrust front of the North Scotia Ridge); ocean bottom seismometer (OBS) position from Schimschal and Jokat (2019); AFFZ - Agulhas-Falkland Fracture Zone; NSR - North Scotia Ridge.

2.2. Architecture of the Falkland Plateau Basin

2.2.1. Structure

The distribution of crustal types under the FPB is still uncertain. The Falkland Islands and the Maurice Ewing Bank were part of a continuous block, as suggested by geochemical and isotopic analyses of their basement lithologies (Thomas et al., 2000; Chemale et al., 2018), which underwent extension and/or potential break-up during the fragmentation of Gondwana (Chemale et al., 2018). Gravity modelling studies (Richards et al., 1996; Kimbell and Richards, 2008) and the interpretation of seismic reflection and refraction data (Ludwig, 1983; Lorenzo and Mutter, 1988) show that the resulting basin is underlain by either thick oceanic crust or thinned and underplated continental crust. Recent studies have revealed more evidence on the presence of oceanic crust in the FPB (Schimschal and Jokat, 2017, 2019; Eagles and Eisermann, 2020) but the extent of the oceanic domain remains uncertain. The results of the refraction study of Schimschal and Jokat (2017, 2019) show the presence of high P-wave velocities indicative of oceanic crust along an E-W trending profile across the FPB (Fig. 1), but with no constraints on the N-S extent of this potential oceanic domain. Similarly, Eagles and Eisermann (2020) present a crustal model of the FPB based on newly-acquired magnetic data where the entire FPB, with the exception of the AFFZ-adjacent area, is interpreted as oceanic or igneous crust. However, magnetic reversal isochrons indicative of typical oceanic crust are present only in the south-eastern part of the basin (Eagles and Eisermann, 2020).

The FPB is bounded to the west by NE-SW trending normal faults that down-throw to the south-east (Richards et al., 1996), and to the east by the Maurice Ewing Bank. Most of the normal faults interpreted from seismic reflection data along the basin terminate at the top Jurassic (Lorenzo and Mutter, 1988). Rifting within the FPB was interpreted to have occurred either between Middle Jurassic and Lower Cretaceous (Lorenzo and Mutter, 1988) or during the Lower Jurassic (Marshall, 1994; Richards et al., 1996), although some authors argue for an earlier onset of rifting during the Permo-Triassic (Richards et al., 1996). No wells penetrated the oldest synrift deposits, rendering the timing of rifting initiation speculative.

2.2.2. Stratigraphy

Gravity modelling and seismic reflection and refraction data interpretation revealed the presence of an up to 12 km thick sediment infill in the FPB (Richards et al., 1996; Schimschal and Jokat, 2017). This sedimentary succession is constrained by well data on the western part of Maurice Ewing Bank (DSDPs 327, 330, 511, 329, and 512) and east of the Falkland Islands (61/05–1, 31/12–1) (Figs. 1 and 2). The remaining part of the basin fill is interpreted on the basis of seismic facies analysis (Ludwig et al., 1983; Del Ben and Mallardi, 2004).

The Middle to Upper Jurassic recorded a relative sea-level rise (Thompson, 1977) that accounted for the deposition of open shelf deposits rich in terrigenous material. Middle Jurassic to Oxfordian sandstones, siltstones, and claystones interbedded with limestones (Barker, 1977) are overlain by Middle Jurassic non-marine sandstones and siltstones with lignitic intervals (Thompson, 1977). From the end of the Jurassic and throughout the Lower Cretaceous up to late Aptian time, claystones and mudstones rich in organic matter and interbedded with micritic limestone were deposited in a restricted basin environment (Barker, 1977; Thompson, 1977; Ludwig, 1983). The Albian, Upper Cretaceous, and the Cenozoic were associated with open marine conditions (Thompson, 1977) and the deposition of pelagic carbonates, zeolitic oozes and clays, and chalk. Throughout the Cretaceous, the western margin of the basin recorded the deposition of deltaic sandstones and

sand-rich deep marine fans intercalated with claystones (BHP Billiton Petroleum, 2010; Falkland Oil and Gas Limited, 2013). Paleocene to Lower Oligocene sediment drift deposits are interpreted in the Cenozoic succession (Lorenzo and Mutter, 1988; Del Ben and Mallardi, 2004) overlain by Pliocene to Recent gravels, siliceous sands, and foraminiferal oozes (Barker, 1977; Ludwig, 1983) (Fig. 2).

Major uncertainty remains on the age of the oldest sediments in the FPB. DSDP 330 cored Middle Jurassic deposits resting on a Precambrian basement (Barker et al., 1977), but older sedimentary rocks are inferred from seismic velocities and gravity modelling with synrift deposition potentially starting in Permo-Triassic (Richards et al., 1996).

Several regional unconformities have been identified on seismic reflection data: a Tithonian to Lower Cretaceous unconformity spanning 30 Myr ('U2' in Lorenzo and Mutter (1988) and 'J' in Del Ben and Mallardi (2004)), a Middle Cretaceous unconformity marked 'U3' in Lorenzo and Mutter (1988), and an unconformity at the Cretaceous/Cenozoic boundary ('U4' in Lorenzo and Mutter (1988) and 'K' in Del Ben and Mallardi (2004)) (Fig. 2).

2.2.3. Volcanism

The break-up of south-western Gondwana was associated with extensive volcanism and magmatism resulting in the formation of the widespread Karroo – Ferrar large igneous province (Encarnación et al., 1996; Macdonald et al., 2003). This event has been related to the emplacement of several dyke swarms identified onshore the Falkland Islands trending predominantly E-W and NE-SW, although a higher variability in orientations has been observed across West Falkland (Aldiss and Edwards, 1999; Mitchell et al., 1999; Stone et al., 2009; Hole et al., 2016; Stone, 2016). E-W and NE-SW trending dykes yielded K-Ar and Ar-Ar ages of 188 ± 2 to 190 ± 4 Ma and 162 ± 6 to 178.6 ± 4.9 Ma, respectively (Mussett and Taylor, 1994; Thistlewood et al., 1997; Stone et al., 2008; Stone et al., 2009), although a maximum age of 193 ± 4 Ma was also obtained for a NE-SW trending dyke (Mussett and Taylor, 1994). An onshore N-S trending dyke swarm varying in age from 121 ± 1.2 Ma to 138 ± 4 Ma (Stone et al., 2008; Richards et al., 2013) has been related to the early opening of the South Atlantic (Stone et al., 2009; Stone, 2016). N-S trending dykes have also been interpreted nearshore the Falkland Islands on magnetic data (Barker, 1999).

Proof of volcanic activity has been invoked in the interpretation of seismic reflection data from the FPB in the form of volcanic edifices and dipping reflectors within the basement (Lorenzo and Mutter, 1988). The presence of the latter was supported by Barker (1999) and Schimschal and Jokat (2017) who correlated potential seaward-dipping reflectors packages with velocities of over 4 km/s. Positive magnetic and gravity anomalies along the western margin of the FPB were also interpreted as being generated by basaltic flows and/or the presence of plutonic bodies (Richards et al., 1996; Barker, 1999) whereas seismic reflection data revealed the presence of sills intruded in the FPB sediment pile and interpreted as Early Cretaceous in age (Richards et al., 2013).

2.3. Falkland Islands Microplate – Current reconstruction models

The evolution and overall structure of the FPB is strongly correlated with the behaviour of the Falkland Islands during the fragmentation of Gondwana. Similarly, the pre-break-up structural grain of the Falkland Islands Microplate was inherited from the Permo-Triassic Gondwanide orogeny, which resulted in WNW-ESE trending folds and thrusts and NE-SW trending folds related to NNE-SSW compression and NE-SW dextral transpression,

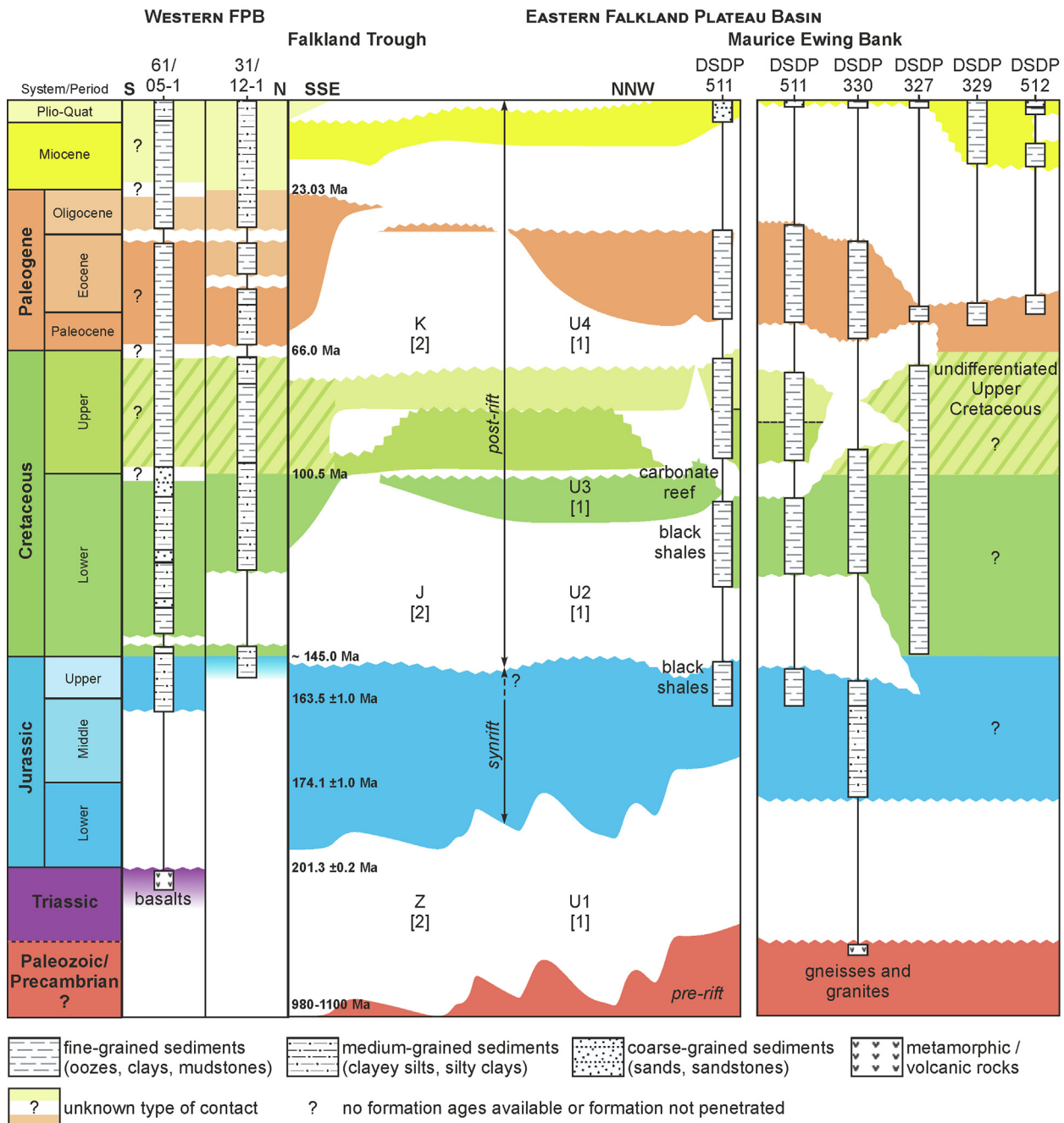


Fig. 2. Chronostratigraphic diagram for the Falkland Plateau Basin based on well data (Western FPB), the interpretation of the seismic reflection profile I95167 from Del Ben and Mallardi (2004) (Eastern FPB), and DSDP information (Eastern FPB and Maurice Ewing Bank; Barker, 1977; Ludwig et al., 1980, 1983; Lorenzo and Mutter, 1988); main unconformities and nomenclature from [1] Lorenzo and Mutter (1988) and [2] Del Ben and Mallardi (2004); unconformities and formation ages along the Western FPB from BHP Billiton Petroleum (2010) and Falkland Oil and Gas Limited (2013); geometries of unconformities along the Eastern FPB redrawn after Del Ben and Mallardi (2004); correlation of unconformities along the Maurice Ewing Bank redrawn after Lorenzo and Mutter (1988); units are colour-coded to reflect their ages; FPB – Falkland Plateau Basin.

respectively (Curtis and Hyam, 1998; Aldiss and Edwards, 1999; Hodgkinson, 2002).

Stratigraphic and structural correlations between the Falkland Islands and South Africa along with fossil assemblages, Late Paleozoic ice flow directions, and palaeomagnetic data analysis have been used to reconstruct a rotated position of the islands in a Gondwana pre-break-up configuration. The angle of rotation between the pre-Jurassic and current day position has been estimated between ~80° and 120°, with an additional ~60° occurring during the opening of the South Atlantic (Adie, 1952; Mitchell et al., 1986; Marshall, 1994; Mussett and Taylor, 1994; Curtis

and Hyam, 1998; Trewin et al., 2002; Stone et al., 2009; Stanca et al., 2019) (Fig. 3). This scenario positions the Falkland Islands off the south-east coast of South Africa, with the basement cropping out onshore the islands representing a fragment of the Namaqua-Natal-Maud belt extending across South Africa and East Antarctica (Thomas et al., 1997; Jacobs et al., 1999; Jacobs et al., 2003; Jacobs and Thomas, 2004; Vorster et al., 2016). A separation between the East and West Falkland reconstruction has been interpreted along the Falkland Sound Fault which has been inferred to run between the two main islands (Fig. 4a; Thomas et al., 1997). However, the sense of movement, displacement, and timing of

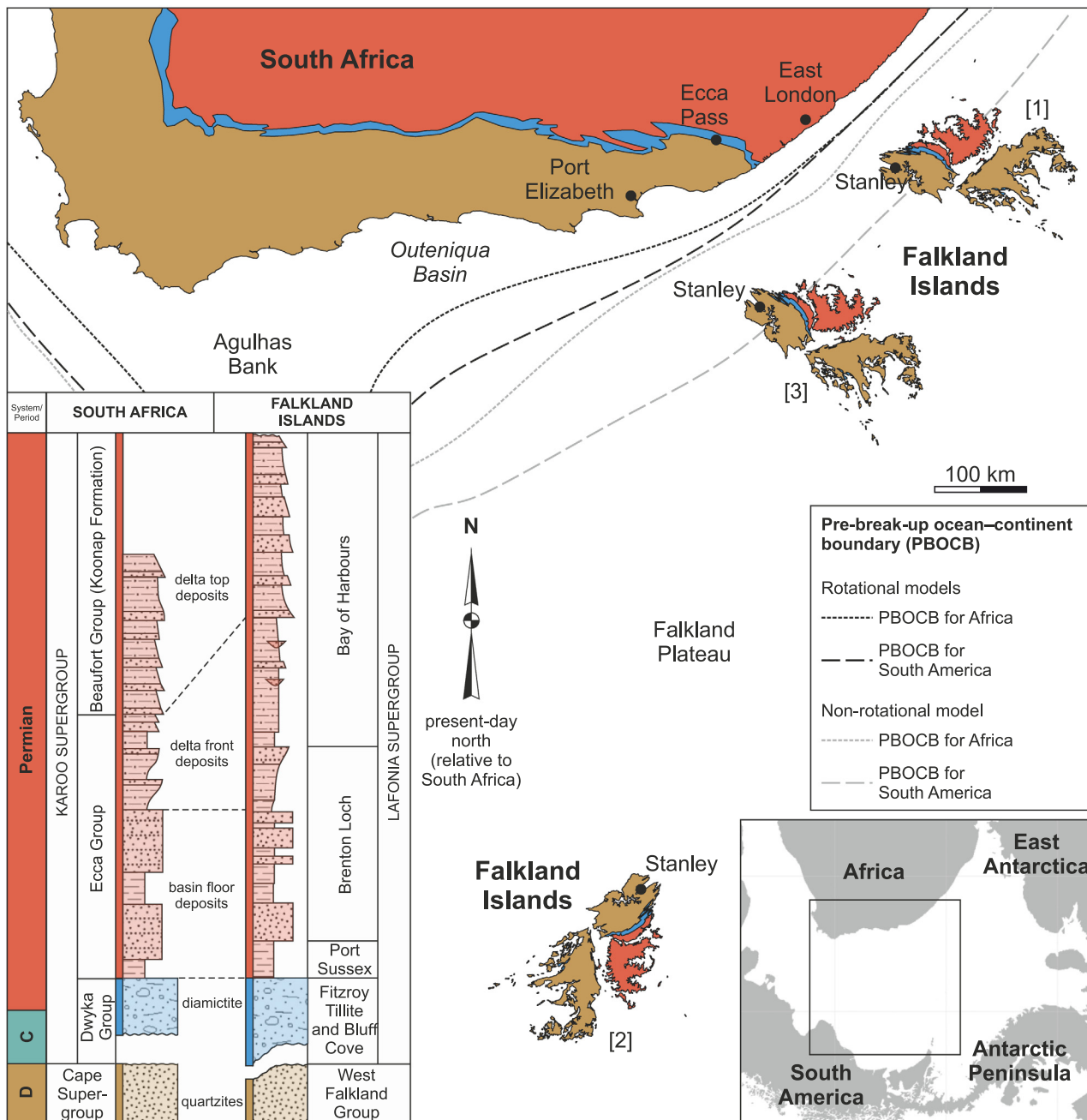


Fig. 3. Jurassic rotational ([1] and [3]) and non-rotational ([2]) reconstruction models of the Falkland Islands after [1] [Trewin et al. \(2002\)](#), [2] [Ramos \(2008\)](#), and [3] [Stanca et al. \(2019\)](#); the stratigraphy and correlation between the Falkland Islands and South African onshore sedimentary deposits is based on [Trewin et al. \(2002\)](#); the PBOCB for the rotational models is based on gravity data and drawn after [Lawver et al. \(1999\)](#) and [Macdonald et al. \(2003\)](#); the PBOCB for the non-rotational model is based on seismic and bathymetric data and drawn after [Martin et al. \(1981\)](#); inset in bottom, right corner shows the south-western configuration of Gondwana after [Müller et al. \(2019\)](#) with Africa fixed in its present-day position.

activity along this major structure have been difficult to constrain ([Marshall, 1994](#); [Richards et al., 1996](#); [Thomas et al., 1997](#); [Curtis and Hyam, 1998](#); [Aldiss and Edwards, 1999](#)).

The rotated reconstruction requires a fragmentation of the FP so that the islands are part of a separate microplate (the FIM) that underwent isolated clockwise vertical-axis rotation. Definition of FIM boundaries is still subject to debate. The microplate is considered to continue north all the way up to the Agulhas-Falkland Fracture Zone by some authors ([Marshall, 1994](#)) whereas others put the boundary further south, along the gravity positive anomaly corresponding to the Southern North Falkland Basin ([Storey et al., 1999](#)) (Fig. 4b, c). Its western extent is interpreted to be marked by the arcuate positive gravity anomaly along the edge

of the Malvinas Basin, and the eastern boundary is thought to coincide with the NE-SW trending positive gravity anomaly ([Storey et al., 1999](#)) (Fig. 4b, c). The minimum southern extent corresponds to the NSR (Figs. 1 and 4b, c).

Studies favouring the rotation of the Falkland Islands argue for a more northern position of the islands relative to South Africa (Fig. 3). This would require significant displacement along a right-lateral fault between Patagonia and the remainder of the South American plate (e. g. Gastre Fault; [Rapela and Pankhurst, 1992](#); [Ben-Avraham et al., 1993](#)) which has been disproved by subsequent studies ([von Gosen and Loske, 2004](#); [Franzese and Martino, 1998](#) in [Ramos et al., 2017](#)). More recent global and South Atlantic reconstructions achieve a closer fit between Patagonia

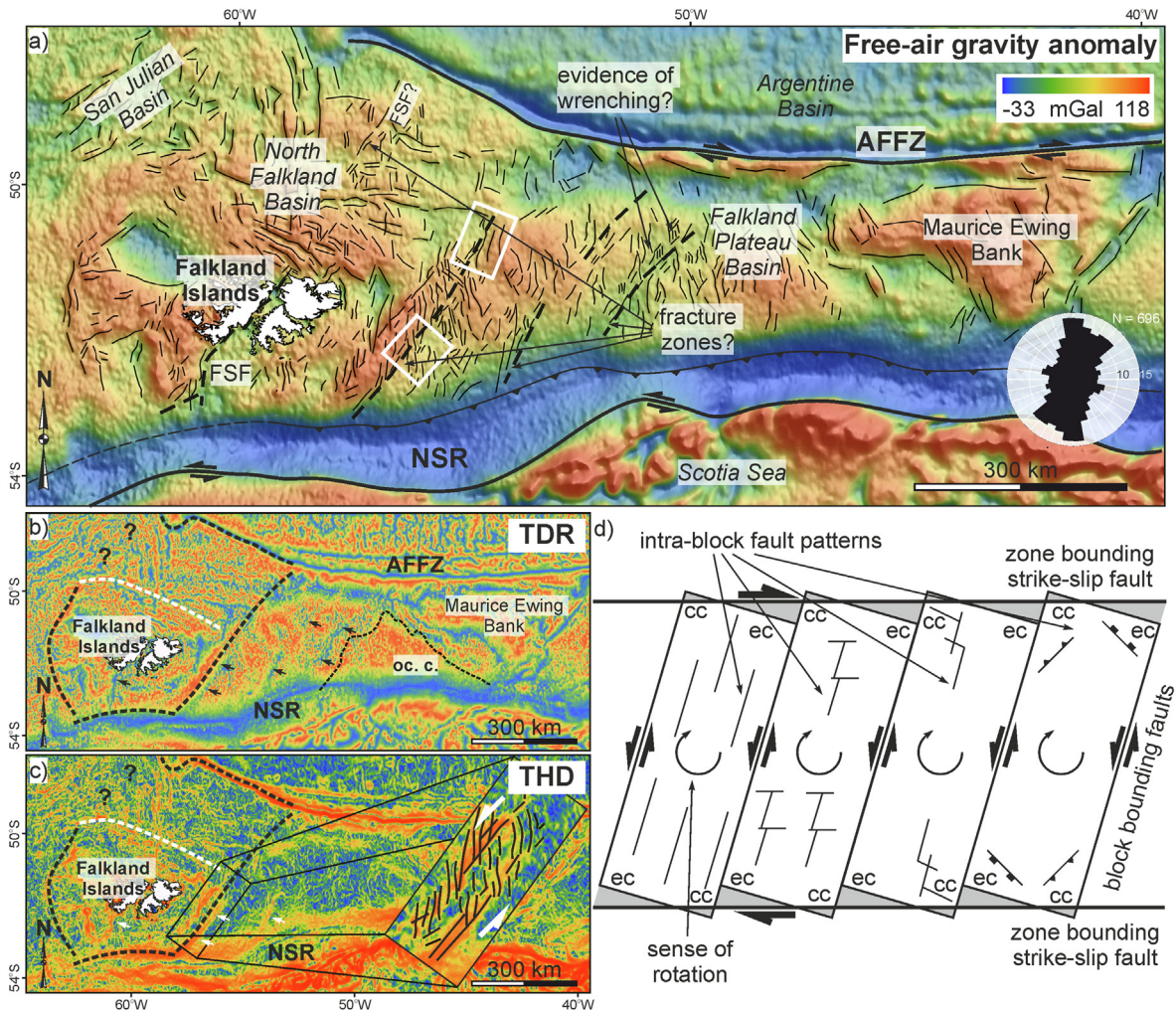


Fig. 4. a) Free-air gravity anomaly (Sandwell et al., 2014) across the Falkland Plateau along with gravity lineaments showing the variation in structural grain; stippled black lines mark potential intra-plate fracture zones accommodating the rotation of the FIM; an area-weighted rose diagram of the mapped features is also shown; white rectangles – seismic cubes; b) tilt derivative (TDR); black arrows show the potential regional fracture zones; c) total horizontal derivative (THD); white arrows show the potential regional fracture zones; inset showing the structural grain along the western margin of the Falkland Plateau Basin; black, thick stippled lines in (b) and (c) mark the potential boundaries of the FIM, white stippled line marks an alternative northern boundary of the FIM after Storey et al. (1999) and black question marks show uncertainties in the location of the western FIM boundary; thin stippled line in (b) mark the extent of magnetic reversal isochrons from Eagles and Eisermann (2020) (oc. c. – oceanic crust); d) map-view of potential intra-block fault networks accommodating block rotation after Peacock et al. (1998); grey areas mark the regions gained and lost during block rotation assuming an original rectangular shape of the blocks; the change in shape is accommodated through intra-block faulting; potential fault patterns that may occur are drawn after Peacock et al. (1998) and are, from left to right: one fault network consisting of faults parallel to the block bounding faults, two fault networks parallel to the block and zone bounding faults, conjugate strike-slip faults in the corners where compression is expected, thrusts and normal faults occurring in the contractional (cc) and extensional (ec) corners, respectively; deformation exhibits a fractal behaviour and block widths vary between 10 mm and 100 km in the model of Peacock et al. (1998); AFFZ – Agulhas-Falkland Fracture Zone; NSR – North Scotia Ridge; FSF – Falkland Sound Fault.

(and the islands) and South Africa by taking into account intra-plate deformation of South America during the fragmentation of Gondwana (Heine et al., 2013; Müller et al., 2019).

The lack of documented deformation in the sedimentary basins offshore the islands (Richards et al., 1996) that would support the rotation, along with the absence of a mechanism for it occurring at the FIM scale, led to several authors favouring a non-rotational evolution model. In this model, the Falkland Islands remain fixed to the South American plate (Fig. 3) throughout the Mesozoic, and the present-day morphology of the FP is either the result of extension coeval with the opening of the South Atlantic (Lawrence et al., 1999; Ramos et al., 2017; Lovocchio et al., 2019; Schimschal and Jokat, 2019) or the plateau represents the conjugate to the Weddell Sea and undergoes extension related to the break-up and drift of the Antarctic plates (Eagles and Vaughan, 2009; Eagles and Eisermann, 2020). Arguments supporting these models are based on stratigraphic and structural correlations car-

ried between the Falkland Islands and Patagonia (Lawrence et al., 1999; Ramos et al., 2017; Chemale et al., 2018; Lovocchio et al., 2019) and magnetic reversal isochrons and magnetic anomaly correlations between the FP on one side, and the Central Scotia Sea and the Weddell Sea on the other side (Eagles and Eisermann, 2020).

3. Data and methodology

3.1. Gravity data and interpretation

The gravity data consist of the V24.1 1-minute satellite altimetry free-air gravity anomaly grid of Sandwell et al. (2014) for the entire FP. Total horizontal (Cordell and Grauch, 1985) and tilt derivatives (Miller and Singh, 1994; Verduzco et al., 2004; Oruç and Keskinsezer, 2008) were computed using Geosoft's Oasis Montaj software and used to map gravity lineaments across the entire

FP (Fig. 4). The nature of the interpreted structures was constrained using seismic reflection data.

3.2. Seismic reflection data and interpretation

The seismic reflection data comprise 2D and 3D survey data (courtesy of the Falkland Islands Government) from seven vintages acquired between 1977 and 2014 by Falklands Oil and Gas Limited, WesternGeco, Noble Energy, Lamont-Doherty Earth Observatory, and Geophysical Service Incorporated (GSI) (Fig. 1). The Falkland Oil and Gas Limited 2D survey from 2007 was the main 2D dataset used for the interpretation due to its resolution and coverage of the western margin of the FPB. It consists of 154 lines with variable spacing on a grid predominantly orientated parallel (NE-SW to ENE-WSW) and sub-perpendicular (WNW-ESE to NNW-SSE) to the shelf (Fig. 1). The record length of this survey is of 8 s TWT, with shot and receiver spacing of 25 m and 12.5 m, respectively. The coverage of this dataset was complemented by 22 lines from the 1993 WesternGeco survey (reprocessed in 2003). These have a record length of 9 s TWT and a shot and receiver spacing of 40 m and 10 m, respectively. Two 3D seismic cubes (FINA along the Berkeley Arch and Volunteer sub-basin and FISA in the Fitzroy sub-basin) aided with the interpretation of smaller scale faults and with the assessments of the 3D distribution of these fault networks and of the magmatic systems. The FINA and FISA cubes cover areas of ~ 5750 km² and ~ 5500 km², respectively, and have record lengths of ~ 9 s TWT. Older regional surveys (two lines from the RC2106 1978 Lamont-Doherty Earth Observatory survey, one line from the 1978 GSI survey, and four lines from the 1977 Western survey) were used for correlations between the western margin of the FPB and the DSDPs on the eastern side. These have record lengths between 4 and 12 s TWT and a poorer data quality compared to the more recent surveys but provided regional information about the basement geometries and the main stratigraphic packages. Five wells (31/12–1, 42/07–1, 61/05–1, 61/17–1, and 61/25–1) and three DSDPs (327, 330, and 511) were tied to the seismic reflection data for the horizon interpretation stage.

Four horizons were mapped across the Fitzroy and Volunteer sub-basins (western part of the FPB) and associated with mega-sequences based on stratal terminations and internal geometries of seismic facies (Mitchum et al., 1977; Hubbard et al., 1985a, b). These horizons are: (1) the Upper Cretaceous Claystone and (2) Valanginian unconformity within the transitional to post-rift section, (3) near top Jurassic as the top synrift, and (4) near top Paleozoic as the top of the pre-rift sequence (Fig. 5). Jurassic deposits were only penetrated by well 61/05–1 and DSDPs 330 and 511, reducing the reliability of correlation of Jurassic strata across the Berkeley Arch and into the Volunteer sub-basin. Volcanic rocks of Triassic (?) age were penetrated by well 61/05–1 (Fig. 2) but their extent remains uncertain.

Wavy low to high amplitude reflectors are readily observed within the pre-rift in the Fitzroy sub-basin and are truncated by a section of relatively constant thickness marked by subparallel to oblique reflectors and areas of transparency (Fig. 5a, c). These deposits are associated with wavy to oblique discontinuous reflectors further north, across the Berkeley Arch and in the Volunteer sub-basin, where the upper part of the pre-rift is characterised by higher amplitudes and semi-continuous reflectors (Fig. 5b, d), which make the differentiation from the overlying Mesozoic sediments challenging.

The main synrift phase was correlated with Jurassic and older deposits. The continuous reflectors within this mega-sequence have very low to high amplitudes and are disrupted in the Fitzroy sub-basin by sub-vertically stacked pockmarks. The deposits up to the Upper Valanginian unconformity record the transitional/sag phase. The latter two sections are crosscut by high amplitude

saucer-shaped bodies. The younger Cretaceous section up to Campanian shows oblique geometries with the Maastrichtian and younger deposits onlapping on the former (Fig. 5).

Isochron maps were computed in order to analyse the migration of the depocentres in the FPB as a response to the tectonic activity and sediment source/input (Fig. 6). Faults were mapped across the Volunteer and Fitzroy sub-basins and the Berkeley Arch. The variance and edge detection attributes were the primary methods used to identify small-scale discontinuities in the seismic reflection data related to normal or oblique-slip faults.

4. Structural and stratigraphic characteristics of the Falkland Plateau Basin from seismic and gravity data

4.1. Basin depocentre migration during Mesozoic

The pre-rift section of the western FPB has been interpreted as folded and faulted strata and correlated with the Siluro-Devonian deposits cropping out onshore the Falkland Islands and unconformably overlain by Permo-Carboniferous deposits. The stratigraphic architecture of the infill overlying these Paleozoic deposits was controlled by the tectonic activity affecting the plateau from Mesozoic and throughout the Cenozoic. The top pre-rift TWT map shows the two depocentres corresponding to the Volunteer sub-basin in the north and the Fitzroy sub-basin in the central area separated by a basement high, the Berkeley Arch (Fig. 6a, b). The top pre-rift to Valanginian isochron shows a similar stratigraphic architecture, with sedimentation confined to the two sub-basins and little to no deposits above the Berkeley Arch. A southward migration of the Fitzroy sub-basin depocentre is visible on the Valanginian – Campanian isochron. The Cenozoic marks the merging of the two sub-basins in the larger FPB with little sedimentation occurring at this point along the south-western and northern margins of the basin (Fig. 6c, d and e).

Locally, the Berkeley Arch and Volunteer sub-basin show a higher variability in their stratigraphic architecture throughout the Jurassic and Cretaceous, which is related to the tectonic structures present in the area (Fig. 6f–i). The TWT map of the pre-rift shows fault-bounded WNW-ESE trending depocentres in the northern part of the Berkeley Arch and within the Volunteer sub-basin (Fig. 6f), and minor NNW-SSE striking depocentres in the central and southern parts of the Berkeley Arch, deepening towards the east (Fig. 6f). A similar distribution is observed for the Jurassic deposits with the Volunteer sub-basin as the main depocentre and little sedimentation occurring above the Berkeley Arch (Fig. 6g). Thermal sag deposits that follow the trend of the underlying fault-controlled depocentres were eroded at the end of the Valanginian particularly in the north-eastern part of the area covered by the seismic cube (Fig. 6h). The Lower Cretaceous sees the erosion of Valanginian deposits along a WNW-ESE direction potentially controlled by further sag along the WNW-ESE faults and/or uplift from the north, which focuses these deposits along the Jurassic depocentres (Fig. 6i). During the Upper Cretaceous, the accommodation space increases northwards with little sedimentation occurring along the Berkeley Arch (Fig. 6d). From Maastrichtian onwards, the FPB is established as the main depocentre (Fig. 6c).

The structural control of the Fitzroy sub-basin is less apparent, the depocentre variation being similar to the one described for the entire western margin of the FPB. Local features characteristic of this sub-basin are represented by post-Valanginian Lower Cretaceous channel systems and shelf-incised canyon-fills (Fig. 7).

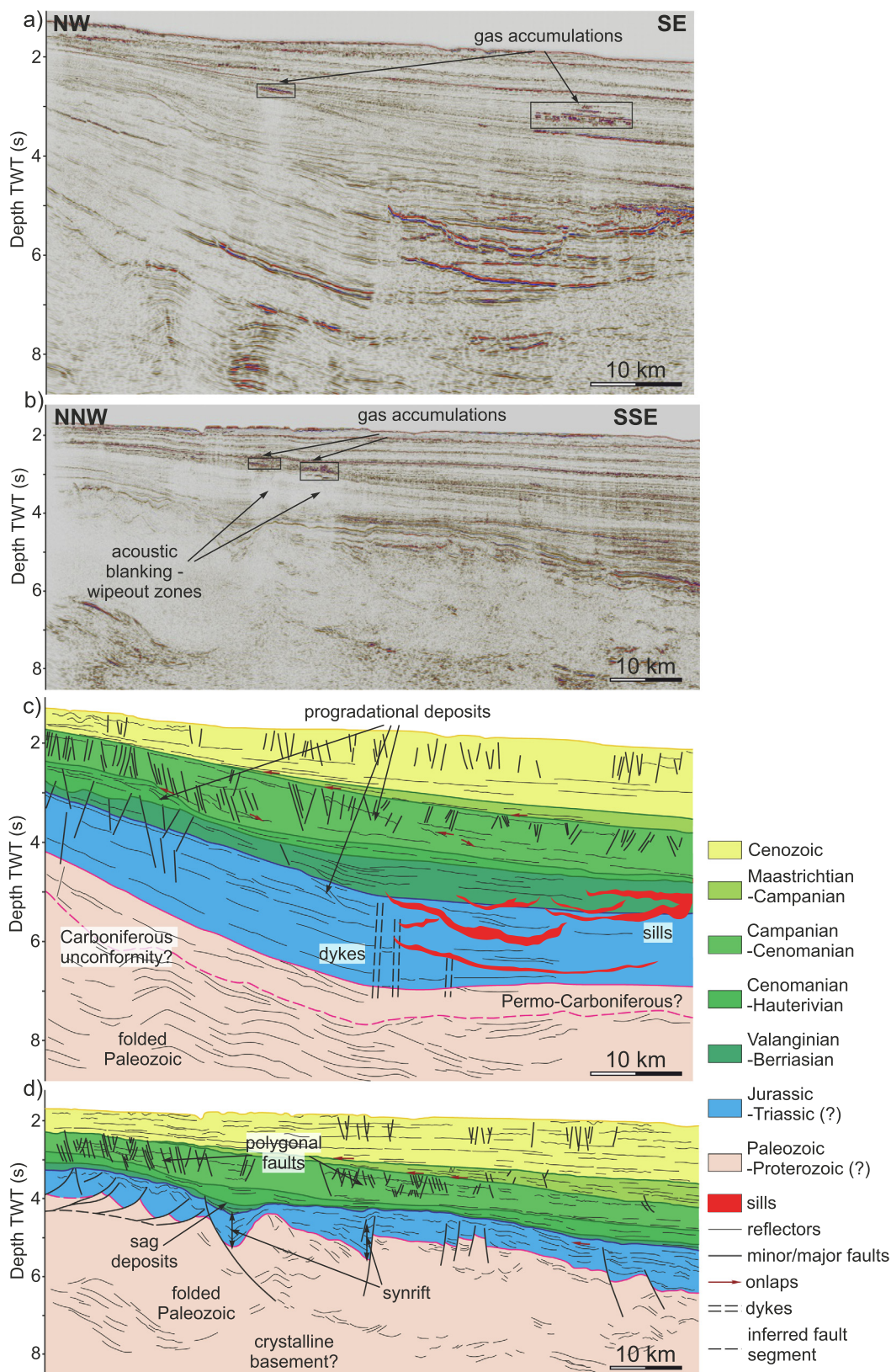


Fig. 5. a) and b) Uninterpreted seismic sections along the Fitzroy sub-basin and the Berkeley Arch, respectively; c) and d) interpreted sections showing the sedimentary sequences, fault network, and evidence of magmatism; lines position shown in Fig. 1.

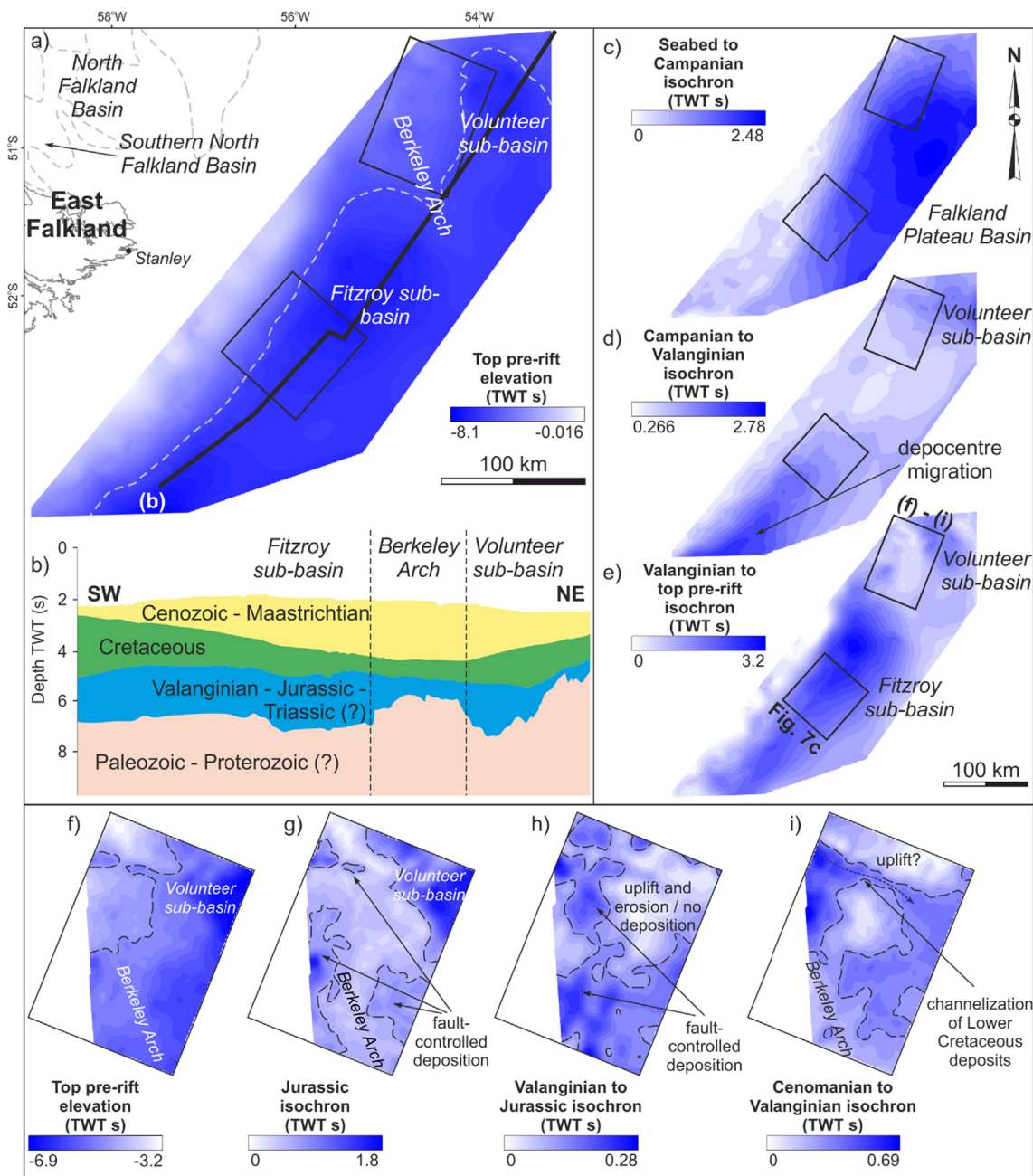


Fig. 6. a) Morphology of the pre-rift topography; b) strike section along the shelf showing the main mega-sequences and basins; c), d), e) thickness maps of the overlying deposits showing depocentre migration as a result of sediment input and tectonism; black rectangles – position of the two 3D seismic cubes; f) top pre-rift TWT map showing the Volunteer sub-basin, WNW-ESE fault-controlled depocentres, and the Berkeley Arch; g) thickness of Jurassic section showing fault controlled deposition; h) thickness of Valanginian-Berriasian deposits showing extensive erosion and fault-controlled depocentres; i) thickness of the Lower Cretaceous section showing uplift from the north controlling the sediment pathway into the basin; location of (f) - (i) shown in (e); black stippled lines – outlines of main depocentres.

4.2. Volcanism and magmatism

Evidence for volcanic activity was identified in both the Volunteer and Fitzroy sub-basins. In the Fitzroy sub-basin, the correlation of vertically or sub-vertically stacked pockmarks (Fig. 8) resulted in a network of N-S trending features showing no evidence of vertical or horizontal displacements. These features are consistent with an interpretation of igneous dykes following the rationale of Magee and Jackson (2019).

Saucer-shaped bodies with high amplitudes and step-like geometries were mapped across the extent of both sub-basins. These are restricted to the Jurassic – Valanginian stratigraphic level and associated with deformation of the surrounding sedimentary

deposits. Their western extent, as constrained by the 2D and 3D seismic reflection data, can be seen in Fig. 11. We interpret these features as sills and their emplacement was associated with the force-folding of the intruded sediments. The relative age for this volcanic event is constrained by onlapping geometries (Fig. 9b, d). Folding of the Valanginian and Aptian-Albian markers and onlap geometries identified in the pre- and post-Valanginian successions indicate an emplacement spanning the Lower Cretaceous. These sills can also be identified above some of the dykes, and we interpret the emplacement of the two as coeval. Locally, the magma feeding the sills and dykes reached the surface resulting in lava flows (Fig. 9b, d, f). Further evidence of volcanism along this margin of the FPB can be seen in the lower section of the Volunteer

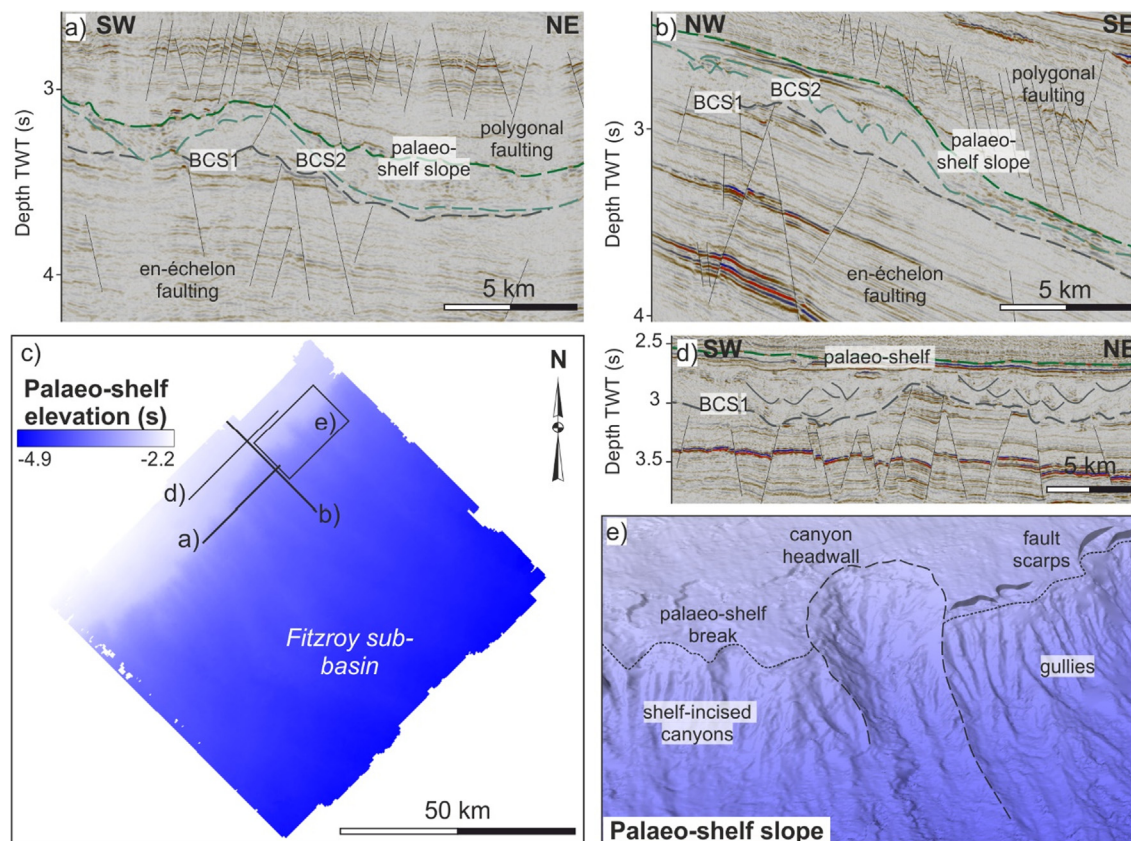


Fig. 7. Evidence for shelf-incised canyons (a, b, d, e) and stacked channels (a, b, d) during the Lower Cretaceous in the Fitzroy sub-basin (southern rectangle in Fig. 6); BCS – base channel system; palaeo-shelf surface in (c) and (e) corresponds to the palaeo-shelf (green dashed line) in (a), (b) and (d). (For interpretation of the references to colour in this figure legend, the reader is referred to the web version of this article.)

sub-basin as high amplitude reflectors (Fig. 13a) interpreted as (pre-)Jurassic volcanic deposits.

4.3. Structural architecture

Three predominant structural trends were identified and mapped across the entire FP with the aid of free-air gravity anomaly data and its computed derivatives and seismic reflection data:

- NW-SE to WNW-ESE: corresponding to the Jurassic SNFB faults, the western margin of the Maurice Ewing Bank and the northern part of the Berkeley Arch (Fig. 4a);
- NE-SW: reflecting the structural grain along the western margin of the FPB, the eastern Maurice Ewing Bank, and the area west of West Falkland; larger scale structures (stippled black lines in Fig. 4a) following the same NE-SW trend were interpreted across the FPB, parallel to the Falkland Sound Fault inferred between the East and West Falkland; a potential continuation of the NE-SW trend of the Falkland Sound Fault can be seen on the gravity data east of the North Falkland Basin (Fig. 4a);
- N-S to NNW-SSE: comprising the Upper Jurassic – Early Cretaceous North Falkland Graben, features in the main FPB and the area west and south-west of the Falkland Islands (Fig. 4a).

This tridirectional structural distribution is evident along the eastern shelf of the FIM. WNW-ESE striking normal faults displace folded Paleozoic deposits and, along the western margin of the FPB, were identified and mapped exclusively in the northern part of the Berkeley Arch (Fig. 10). NNE-SSW striking normal faults affect the rest of the basement high, the Volunteer sub-basin, and are inferred to control the entire western margin of the Fitzroy sub-

basin (Fig. 10). The *syn*-kinematic deposits associated with both fault sets are predominantly Jurassic (Fig. 12) and are consistent with an alternation between almost orthogonal extension directions resulting in the formation and reactivation of NNE-SSW and WNW-ESE striking faults (Figs. 10 and 12).

N-S to NNW-SSE trending normal faults are interpreted along the entire western margin of the FPB and are distributed in either a left- or right-stepping en-échelon geometry (Fig. 14a–e). The faults in this set have small displacements and are restricted to either the Jurassic section along the Berkeley Arch (Fig. 14f) or off-set the Valanginian unconformity in the Fitzroy sub-basin and the northern part of the Berkeley Arch (Fig. 14f, g). Although these normal faults are predominantly interpreted on the 3D seismic reflection data, a similar trend can be observed on the gravity data, at a larger scale, along the western margin of the FPB (Fig. 4c) and locally along the more eastern interpreted fracture zones (Fig. 4a).

Evidence of localized compression in the form of periclinal folds and WNW-ESE trending reverse faults with lengths of up to 4 km can be seen in the Volunteer sub-basin and along the Berkeley Arch, respectively (Fig. 13). These are restricted to the Jurassic level (Fig. 13a, b), albeit a small degree of deformation of the Valanginian marker is noticeable along some of the inverted fault segments (Fig. 13c). Locally, reverse faults reactivate or displace Jurassic WNW-ESE trending normal faults, suggesting a younger relative age for the compression event (Fig. 13b, c).

The post-Valanginian up to present-day section is relatively undeformed with the exception of polygonal faulting (Fig. 5c, d, Fig. 12b).

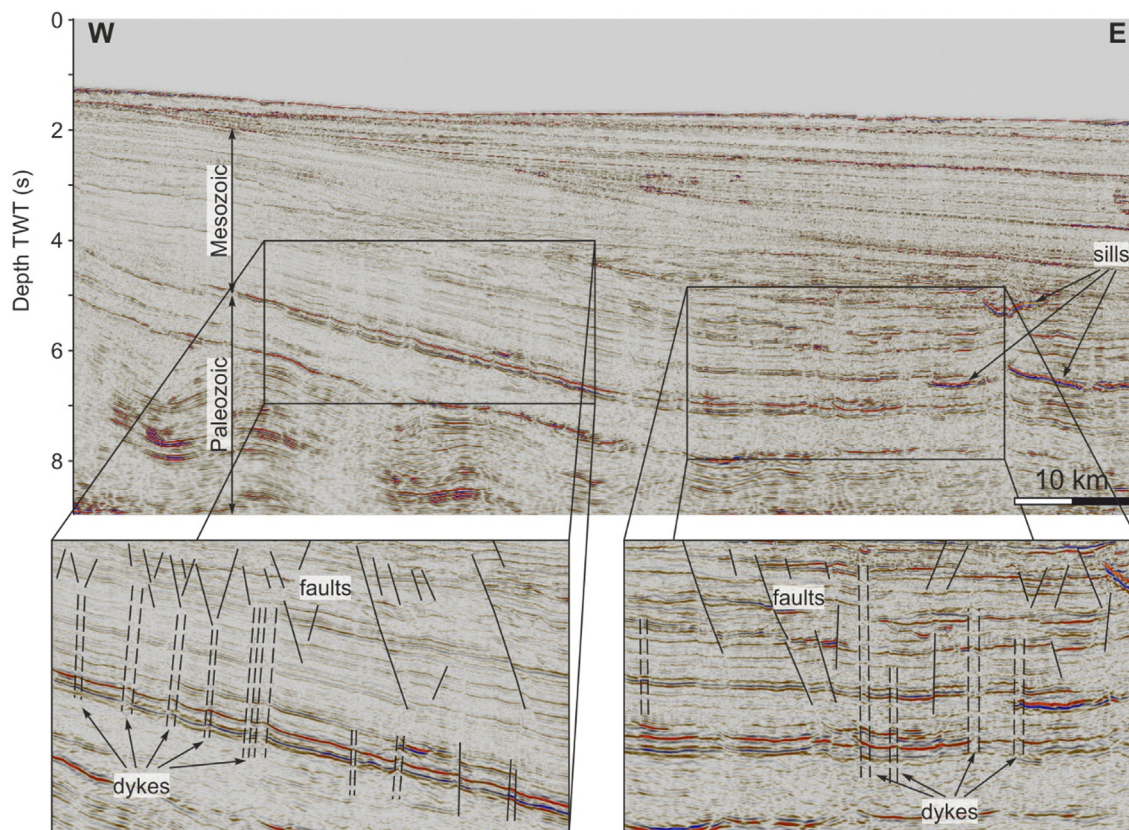


Fig. 8. Pockmarks interpreted as dykes (stippled lines) in the Fitzroy sub-basin; line position shown in Fig. 1.

5. Discussion

5.1. The evolution of the western Falkland Plateau Basin

The present-day morphologies of the Volunteer and Fitzroy sub-basins are the result of extension along the Falkland Plateau associated with the fragmentation of Gondwana and the opening of the South Atlantic. They were further influenced by the movement along the AFFZ and the formation of the NSR. The contrasting structural frameworks and stratigraphic architectures of the two constituent sub-basins point towards different tectono-stratigraphic histories.

The Volunteer sub-basin and the Berkeley Arch show extensive deformation of Paleozoic deposits with two sets of normal faults subdivided based on their orientation: one trending NE-SW and one WNW-ESE (Fig. 10). The synrift deposits show that NW-SE directed extension both preceded and followed the formation of the WNW-ESE trending fault set (Fig. 12), although an alternation between WNW-ESE and roughly NE-SW extension is more likely (Figs. 15, 16). On the free-air gravity anomaly map (Fig. 4a), the WNW-ESE trend correlates with the reactivated faults from the SNFB, suggesting a coeval rifting stage during the Jurassic (Lohr and Underhill, 2015; Stanca et al., 2019). One can argue for an onset of extension synchronous to the emplacement of the Lower Jurassic onshore E-W trending dykes (188 ± 2 to 190 ± 4 Ma; Mussett and Taylor, 1994; Ramos et al., 2017; Fig. 16a). Extension perpendicular to the western NE-SW trending margin of the FPB potentially started during the Lower to Middle Jurassic when dykes following the same trend were emplaced onshore the Falkland Islands (162 ± 6 to 178.6 ± 4.9 Ma; Thistlewood et al., 1997;

Stone et al., 2008; Fig. 15a, Fig. 16b). Variations in the configuration of stress components are seen throughout the Jurassic, resulting in N-S trending en-échélon normal faults superimposed on the first generations of faults (Fig. 14b), and suggestive of secondary sinistral and dextral shearing along NE-SW and WNW-ESE directions, respectively. Locally, evidence of (Upper?) Jurassic compression and positive inversion are seen in the Volunteer sub-basin (Fig. 13). Although the deposition of the Cretaceous and younger sections shows some control of the underlying structures (Fig. 6h, i), the only active faults at this level are polygonal (Fig. 5b, d, Fig. 12b) with evidence of restricted WNW-ESE dextral shearing occurring in the northern part of the seismic cube from this area (Fig. 14b, f) during the Lower Cretaceous.

In contrast, the Fitzroy sub-basin shows little faulting of the Paleozoic deposits, the depth of its depocentre pointing towards subsidence due to loading as a result of a high input of sediments rather than crustal thinning. Discrete faulting could occur basinward, underneath the sills where the seismic imaging is poor (Fig. 5a, c). Localized evidence of Jurassic faulting is interpreted along the shelf (Fig. 10). However, the faulting within the sub-basin is restricted to the Lower Cretaceous interval when N-S to NNW-SSE normal faults are generated with intrusion of dykes that follow the same trend (Fig. 14c- e and g). The en-échélon distribution of these faults suggests a sinistral strike-slip component. The extensive formation and filling of submarine canyons and channels in the Fitzroy sub-basin (Fig. 7) suggest an increase in sediment supply during the Hauterivian-Albian, and/or a relative sea-level fall (Covault, 2011) which might be related to a larger scale isostatic adjustment.

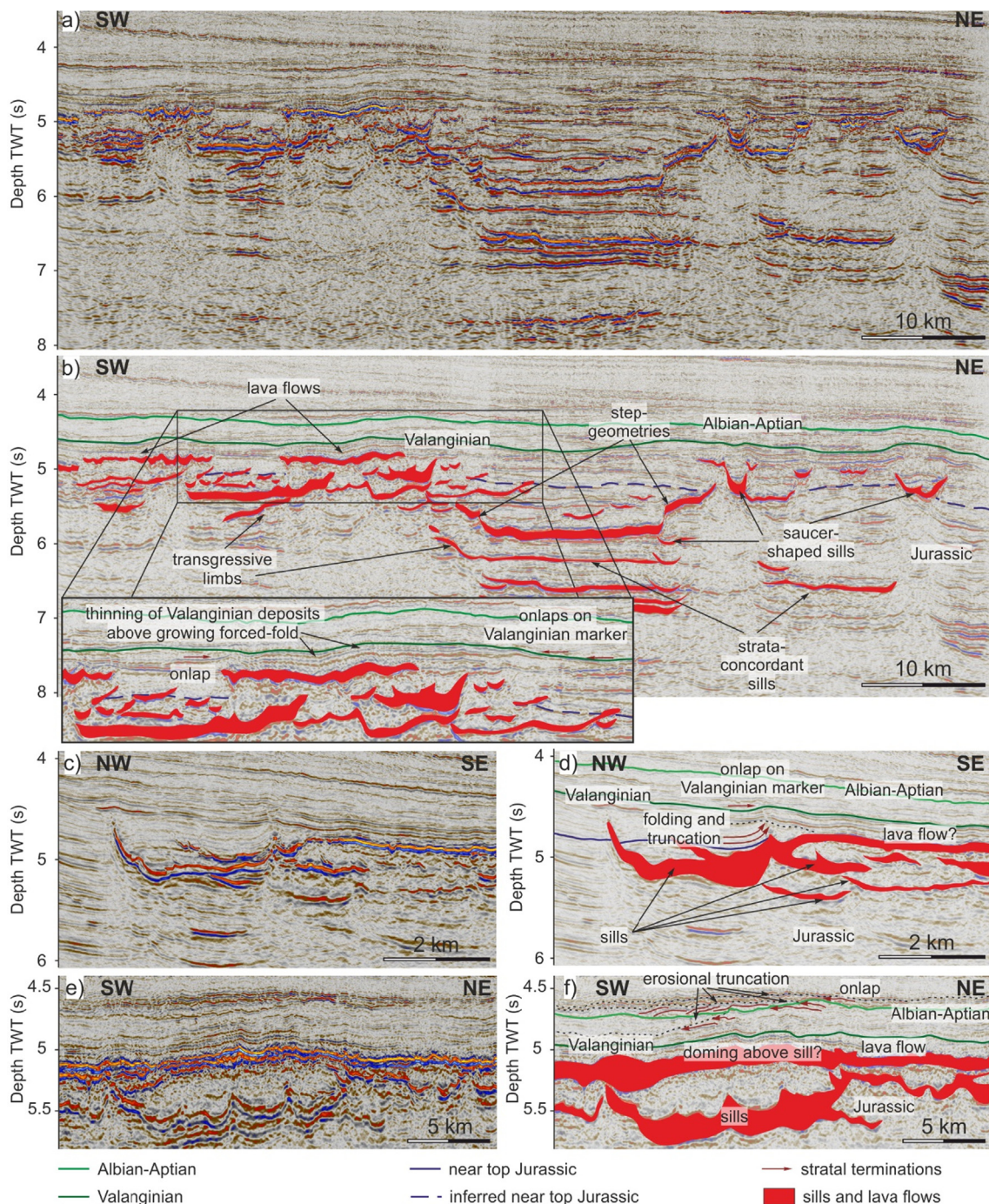


Fig. 9. Sills and lava flow distribution and associated forced-folds in the Fitzroy sub-basin; a) uninterpreted strike line; b) interpretation of section in (a) showing lava flows and sill geometries and extent, and pre- and post-Valanginian evidence of forced-folding coeval with the sills emplacement; c) uninterpreted dip line; d) interpretation of section in (c) showing folding and truncation above the Jurassic marker and in the post-Valanginian section; e) uninterpreted strike line; f) interpretation of section in (e) showing erosional truncation and onlapping below and above the Aptian-Albian marker; lines position shown in Fig. 1.

Although small-scale faults control the stratigraphic architecture in the study area, the overall morphology of the FPB was strongly impacted by the large-scale tectonism, such as movement along the AFFZ and the formation of the NSR. The wrenching and active transform motion period of the AFFZ, as documented on the South African side, occurred between 134 and 92 Ma (Valanginian - Turonian) and resulted in a gradual westward migrating uplift in the Outeniqua Basin (Baby et al., 2018). In the Volunteer sub-basin, the deposition of the Valanginian-Cenomanian

sequence is focused along a WNW-ESE direction (sub-parallel to the AFFZ) and onlaps onto the Valanginian deposits, which could suggest uplift from the north, along the AFFZ (Fig. 6i). A large-scale unconformity is interpreted along the South African margin during the Aptian-Albian (McMillan, 2003; Baby et al., 2018) and related to large scale tectonic events that could explain the canyon incision seen at this time along the western margin of the FPB (Fig. 7).

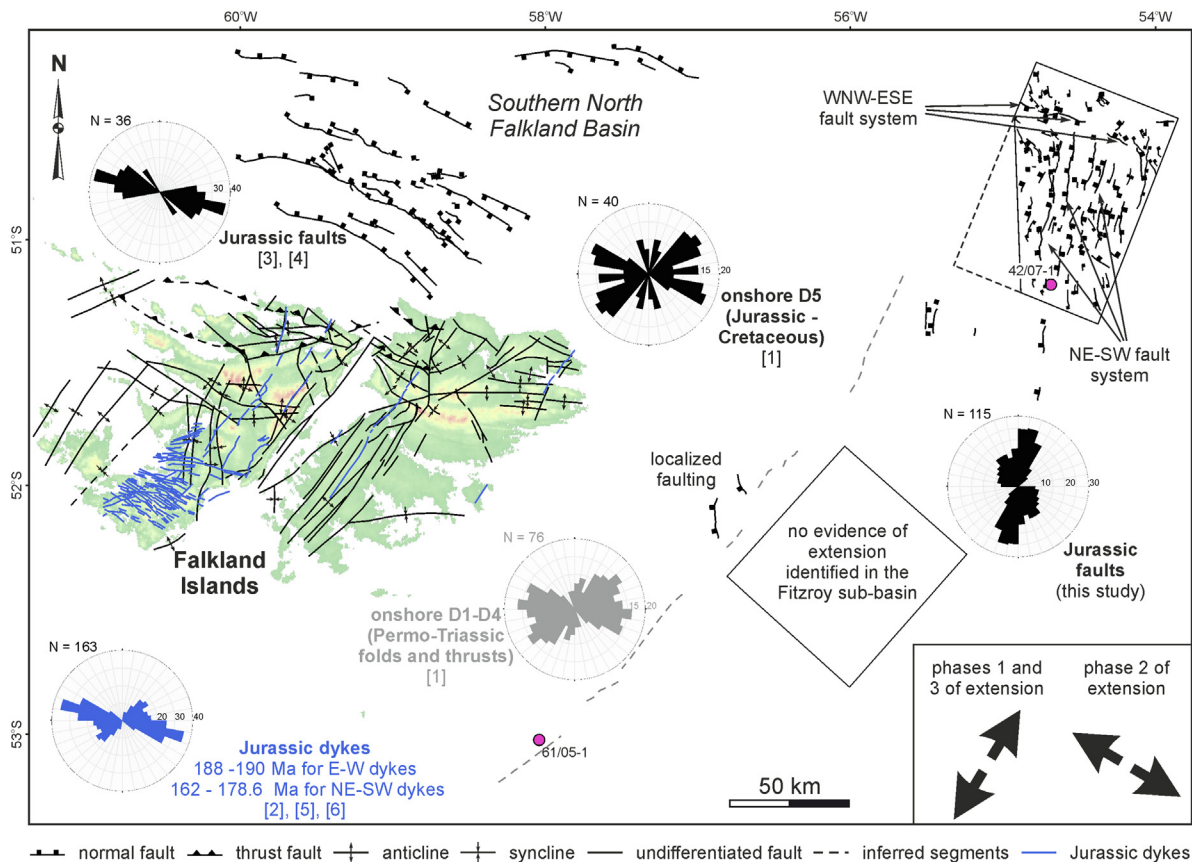


Fig. 10. Compiled Jurassic structural map of the Falkland Islands on- and offshore areas ([1] Aldiss and Edwards, 1999; [2] Stone et al., 2009; [3] Lohr and Underhill, 2015; [4] Stanca et al., 2019, and this study) along with area-weighted rose diagrams for every deformational stage and fault network, showing extension directions throughout Jurassic assumed to be perpendicular on the onshore dyke swarms and offshore normal faults; ages of onshore dykes after [5] Mussett and Taylor (1994) and [6] Stone et al. (2008); arrows show extension direction and their orientation is equivalent to the orientation of σ_3 ; rectangles – location of 3D seismic data.

Compression and uplift along the NSR are thought to have started in the Upper Cretaceous (Bry et al., 2004), which resulted in the southward tilt of the Falkland Plateau (Ewing et al., 1971). This is expressed as a south-eastward increase in accommodation space during this time in the FPB (Fig. 6c).

5.2. Mesozoic structural evolution of the Falkland Islands Microplate

The seismic reflection data interpreted along the western boundary of the FPB does not show a crustal scale feature that could be associated with the eastern boundary of the FIM (Fig. 5). Furthermore, the deformation related to wrenching suggests little sinistral displacement along what was interpreted to be the margin of the microplate (Fig. 14). Therefore, we consider the region comprising the Fitzroy and Volunteer sub-basins as part of the FIM, and that the NE-SW trending gravity anomalies interpreted as fracture zones (Fig. 4a, b and c) accommodate the intra-plate deformation during rotation of the FIM, with the easternmost fracture zone potentially acting as the eastern FIM boundary.

Subsequent to the Gondwanide orogeny, which resulted in WNW-ESE trending folds and thrusts and NE-SW trending folds across the FIM (Curtis and Hyam, 1998; Aldiss and Edwards, 1999), the incipient stages of continental fragmentation resulted in a complicated fault network affecting the microplate. Situated between three major plates, the microplate underwent faulting and dyke emplacement related to the undocking and drifting of East Antarctica and South America away from Africa (Fig. 15).

During the Lower Jurassic, the early stage of Karoo-Ferrar magmatism was marked by WNW-ESE to W-E oriented dyke intrusion in the southern part of West Falkland (188–190 Ma). This was followed by NW-SE directed extension resulting in the emplacement of another dyke swarm (162–179 Ma) onshore the islands, assuming dyke intrusion occurred perpendicular to σ_3 . This stage was potentially synchronous with normal faulting in the Volunteer sub-basin and along the Berkeley Arch (Fig. 16a, b). The Middle (?) - Upper Jurassic sees a rotation in the extension direction to NNE-SSW allowing for the reactivation of the Permo-Triassic thrusts in an extensional regime seen both in the Southern North Falkland Basin and the Volunteer sub-basin (Fig. 16c, d). The structural inheritance given by the presence of older WNW-ESE trending thrusts does not require the extension direction to be perpendicular to these thrusts in order for them to reactivate. Experimental studies on oblique rifting show that pre-existing structures can reactivate with a predominantly normal dip-slip component for angles between 45° and 135° between their trend and the extension direction (Withjack and Jamison, 1986; Henza et al., 2010). For angles outside this range, oblique-slip or strike-slip faults tend to develop (Withjack and Jamison, 1986; Henza et al., 2010). The reactivated thrusts in the SNFB show predominantly normal displacements to oblique-slip (Richards et al., 1996; Lohr and Underhill, 2015; Stanca et al., 2019) suggesting an extension direction between NNW-SSE and NE-SW which would allow multiple stages of movement along these faults throughout the Jurassic (Fig. 16a, c and d).

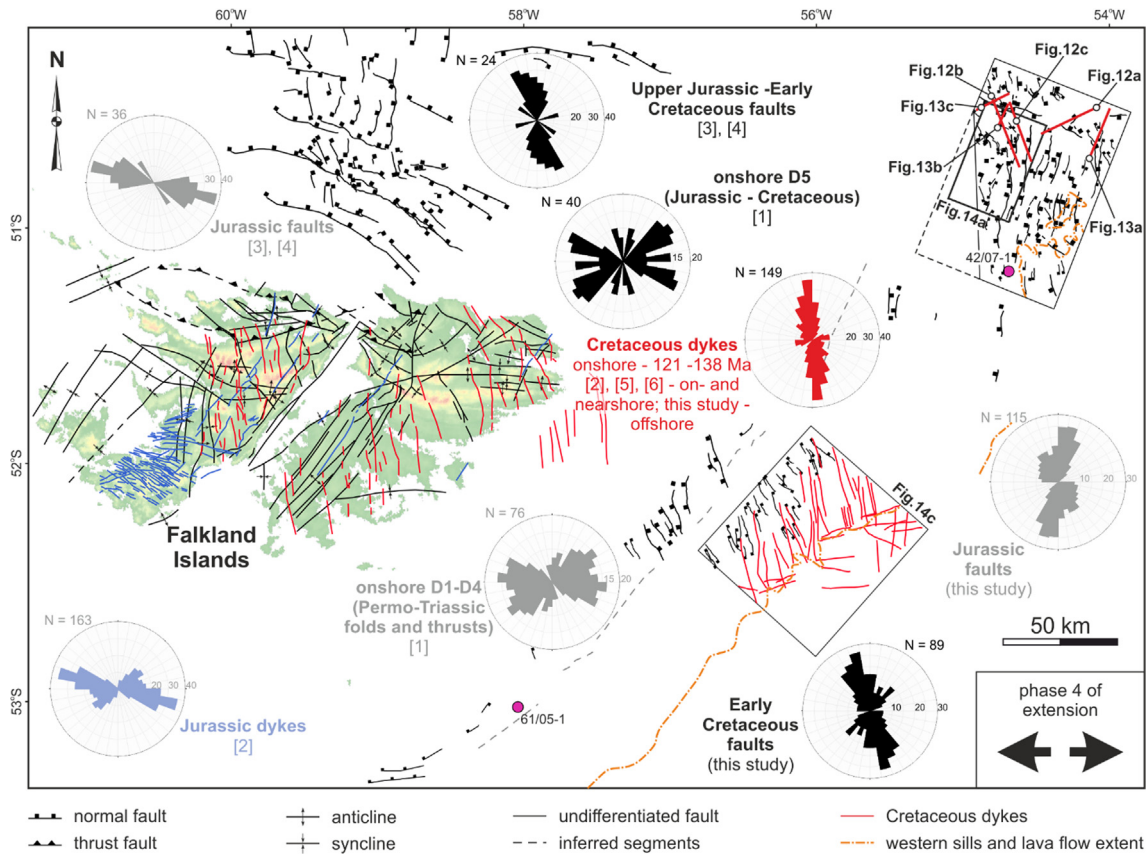


Fig. 11. Compiled Cretaceous structural map of the Falkland Islands on- and offshore areas ([1] Aldiss and Edwards, 1999; [2] Stone et al., 2009; [3] Lohr and Underhill, 2015; [4] Stanca et al., 2019, and this study) along with area-weighted rose diagrams for every deformational stage and fault network, showing extension direction during Cretaceous assumed to be perpendicular on the onshore dyke swarms and offshore normal faults and dykes; ages of onshore dykes after [5] Stone et al. (2008) and [6] Richards et al. (2013); arrows show extension direction and their orientation is equivalent to the orientation of σ_3 ; rectangles – location of 3D seismic data.

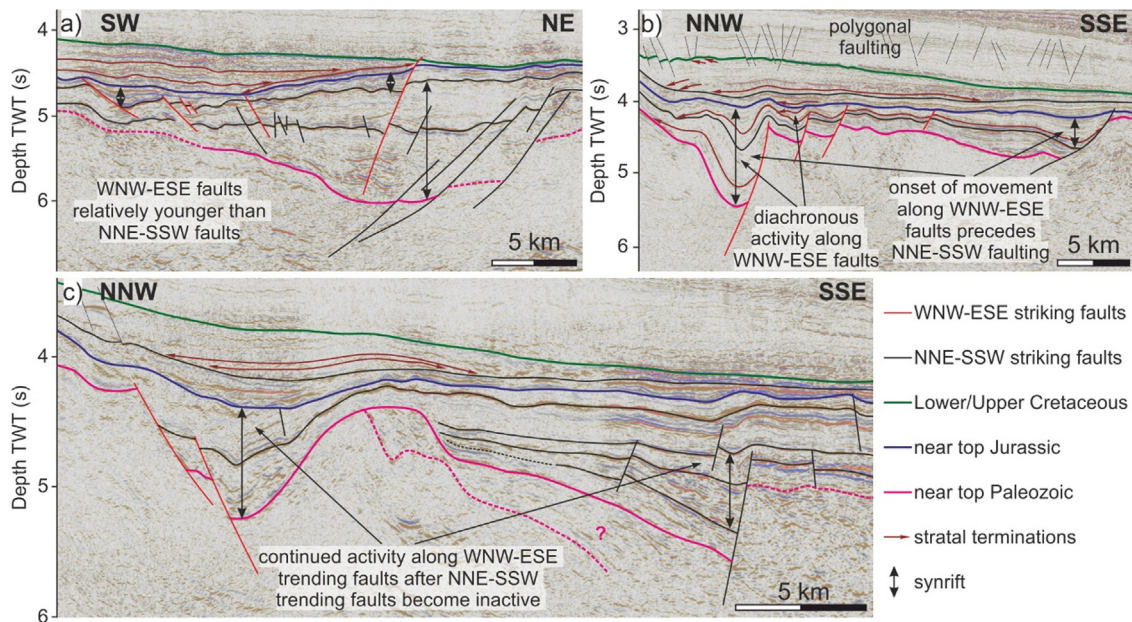


Fig. 12. Relative ages of the WNW-ESE and NNE-SSW trending normal faults in the Volunteer sub-basin and along the Berkeley Arch showing a secondary separation of the same-strike faults based on their ages; motion on NNE-SSW trending faults occurs both before and after the formation on the WNW-ESE trending faults, but both sets are restricted to the Jurassic interval; lines position shown in Fig. 11.

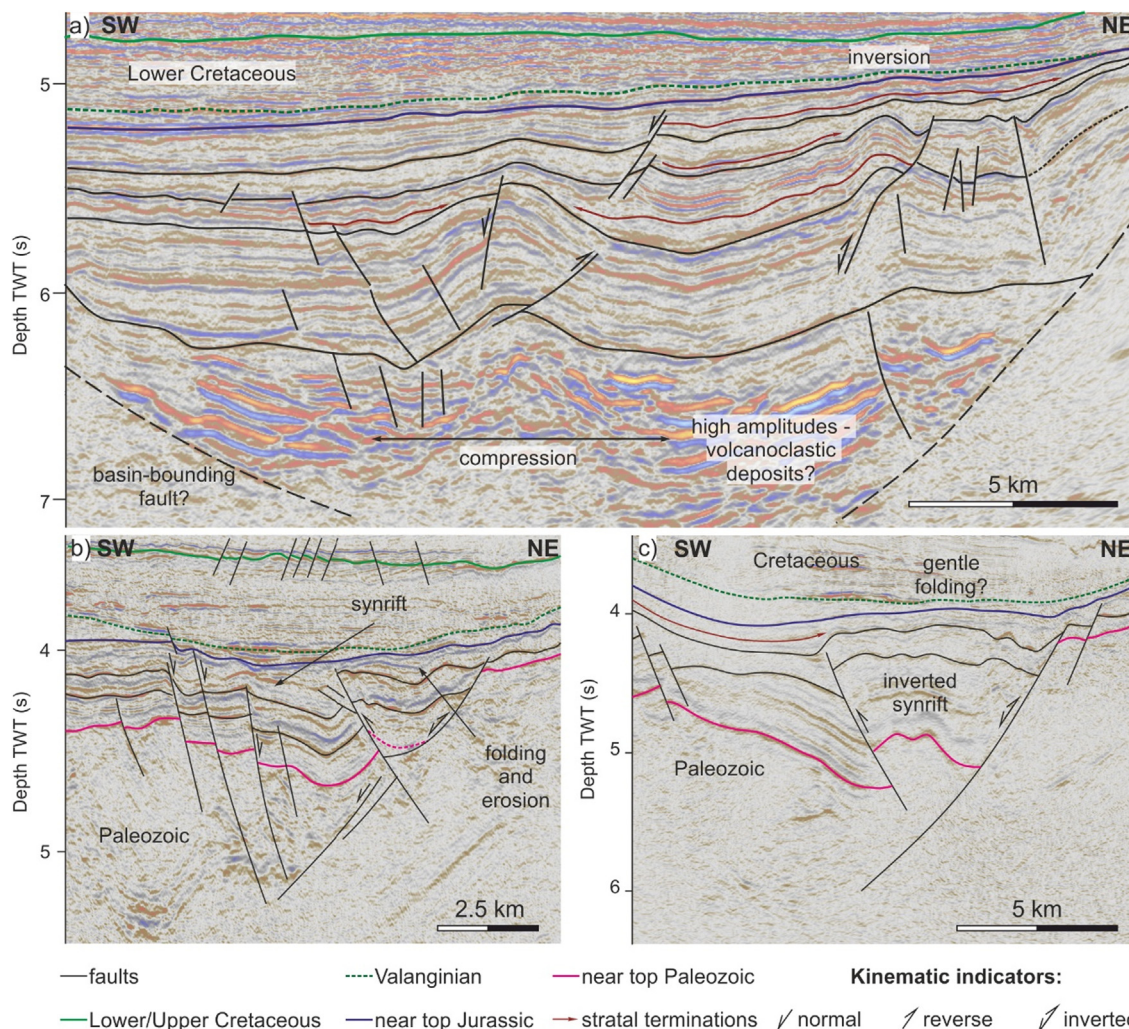


Fig. 13. Evidence for compression/positive inversion in the Volunteer sub-basin in the form of folds and reverse faults; sense of movement for the hanging-wall of the faults indicated; onlaps on folds shown as syn-kinematic indicators; lines position shown in Fig. 11.

Jurassic en-échelon faulting along the margin of the FPB (Fig. 14a, b) is consistent with sinistral and dextral wrenching generated by a NE-SW oriented σ_3 (Fig. 14h and Fig. 16c, d). However, the predominantly small displacements associated with these faults along with the lack of age constraints for the Jurassic section make their relative dating in the context of SNFB rifting difficult. From the end of the Jurassic and into the Lower Cretaceous σ_3 oscillates around a roughly E-W orientation, leading to the opening of the North Falkland Basin, normal faulting in the Fitzroy sub-basin, and the onshore and offshore emplacement of a Lower Cretaceous generation of dykes between 121 ± 1.2 Ma to 138 ± 4 Ma (Fig. 16e, f). Sinistral and dextral shearing occurs at this time locally, along the western margin of the FPB (Fig. 14c, d, e) and in the northern part of the Berkeley Arch (Fig. 14b), respectively, potentially related to the onset of wrenching along the AFFZ (at 134 Ma; Baby et al., 2018). However, these right and left-stepping en-échelon faults could represent reactivated Jurassic structures that accommodated the FIM intra-plate deformation during its rotation, in a similar way to the NE-SW trending regional fracture zones (Fig. 4a) but on a much smaller scale (Peacock et al., 1998; Fig. 4d).

5.3. Stress orientation variation across the FIM in the context of Gondwana

5.3.1. Plate model considerations

In the context of a pre-break-up configuration of south-western Gondwana, the stress variation interpreted across the FIM could help constrain the timing of microplate rotation. This can be done by comparing structures of similar age identified across south-western Gondwana with the aforementioned structural framework. To do this, we used a modified version of the South Atlantic reconstruction after Müller et al. (2019) with Africa fixed to its present-day position. We consider the Falkland Plateau to consist of two sub-plates: the FIM and the Maurice Ewing Bank region. The FIM is defined as the area bounded to the north, west, and south by the black stippled lines in Fig. 4b, c and extends eastward up until the magnetic stripes from Eagles and Eisermann (2020) (oc. c. region in Fig. 4b, c). These were interpreted as magnetic reversal isochrons associated here with the presence of oceanic crust, although a more extensive oceanic domain has been interpreted by Schimschal and Jokat (2019) based on P-wave velocities (black dots in Fig. 1) and by Eagles and Eisermann (2020) based on magnetic data. The Maurice Ewing Bank sub-plate represents the remainder of the plateau. The amount of rotation for the Falkland Islands Microplate during the Lower Jurassic is after Stanca et al.

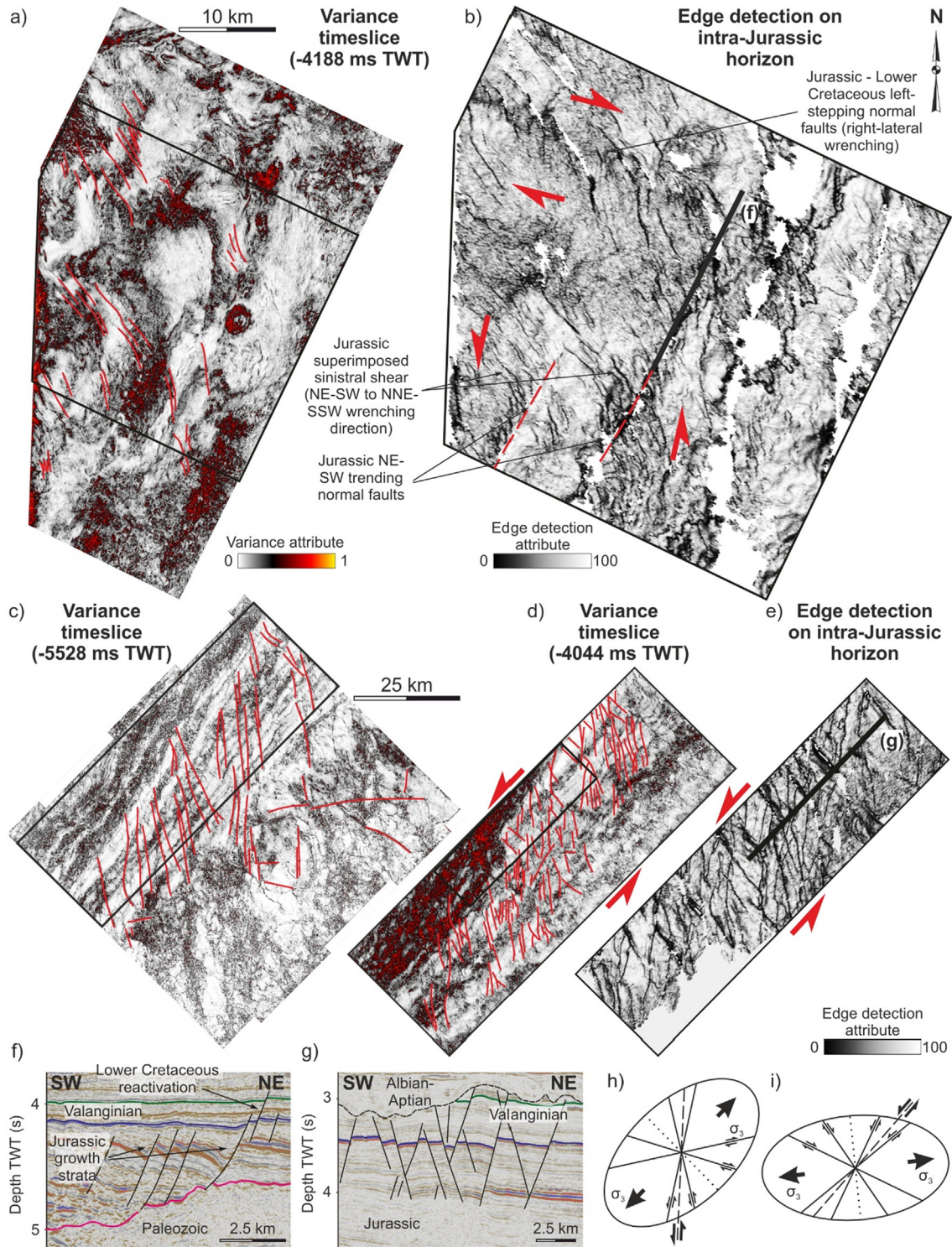


Fig. 14. a) Variance timeslice across the Berkeley Arch showing the distribution of en-échelon faults; black polygon – inset in (b); b) edge detection attribute along an intra-Jurassic horizon showing right and left-stepping en-échelon fault networks; c) faults and dykes distribution on the 3D seismic in the Fitzroy sub-basin; black rectangle - inset in (d); d) en-échelon faults and the sense of shear estimated from their orientation; black rectangle – inset in (e); e) edge detection attribute along an intra-Jurassic horizon showing the complex fault and fracture network generated by sinistral wrenching; f) section through the en-échelon faults in (b); g) section through the en-échelon faults in (e); h) strain ellipse with the orientation of the minimum horizontal stress for (a) and (b); i) strain ellipse with the orientation of the minimum horizontal stress for (c), (d) and (e); direction of arrows mark extension direction and their orientation is equivalent to the orientation of σ_3 ; position of timeslices in (a) and (c) shown in Fig. 11.

(2019) but its exact location remains debatable. Here we position the islands further south than Stanca et al. (2019) in order to eliminate the space between the FIM and South America in the Jurassic reconstruction while not invoking dextral movement along the

Gastre Fault. A more northern position could be accomplished by further deformation of the South American plate. We do not address these scenarios here; rather, the sole aim of the reconstruction is to carry out a qualitative comparison between the

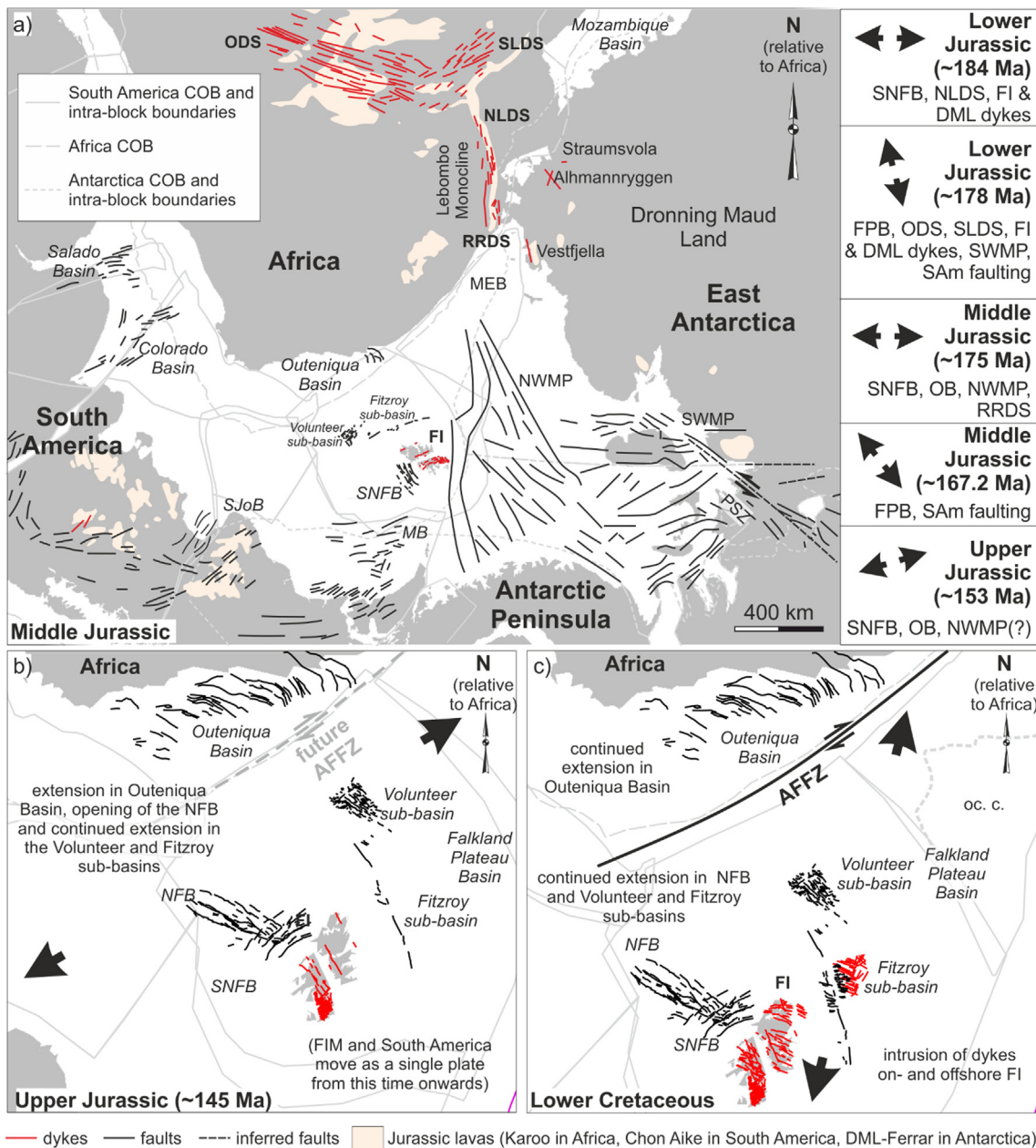


Fig. 15. Correlation between the position of the Falkland Islands and south-western Gondwana based on the orientation of σ_3 for a rotated reconstruction of the FIM; a) Middle Jurassic plate configuration showing the change in the regional orientation of σ_3 from Lower to Upper Jurassic (right panel) and the structural features used for its estimation; b) NE-SW extension direction (Paton and Underhill, 2004) and plate configuration during Upper Jurassic; c) NNE-SSW directed extension (Paton and Underhill, 2004) marked by the emplacement of now N-S trending Early Cretaceous dykes on- and offshore the Falkland Islands; rotation of the FIM after Stanca et al. (2019); the Falkland Islands Microplate and the South American plate rotate clockwise with the remaining $\sim 60^\circ$ during the opening of the South Atlantic (Mitchell et al. 1986) to reach their present-day position; onset of wrenching along the Agulhas – Falkland Fracture Zone after Baby et al. (2018); FI – Falkland Islands; MB – Malvinas Basin; NFB – North Falkland Basin; NLDS – Northern Lebonbo dyke swarm; NWMP – Northern Weddell Magnetic Province; OB – Outeniqua Basin; oc. c. – oceanic crust (based on magnetic reversal isochrons from Eagles and Eisermann, 2020); ODS – Okavango dyke swarm; PSZ – Pagano Shear Zone; RRDS – Rooi Rand dyke swarm; SJoB – San Jorge Basin; SLDS – Save Limpopo dyke swarm; SWMP – Southern Weddell Magnetic Province; SWMP and NWMP framework from Jordan et al. (2017); South Africa simplified dyke network drawn after Gomez (2001); East Antarctica dykes drawn after Curtis et al. (2008); Falkland Islands onshore and nearshore dykes drawn after Stone et al. (2009); Outeniqua Basin fault network after Paton et al. (2006) and Parsieglia et al. (2009); SNFB and NFB fault networks after Lohr and Underhill (2015) and Stanca et al. (2019); South America fault network after Lovocchio et al. (2019); Karoo lavas extent after Jourdan et al. (2007); Chon Aike lavas extent after Bouhier et al. (2017); DML-Ferrar lavas extent after Elliot (1992) and Elliot et al. (1999); arrows show extension direction and their orientation is equivalent to the orientation of σ_3 .

stress fields and structures across the FIM and south-western Gondwana. Similarly, Schimschal and Jokat (2017, 2019) and Eagles and Eisermann (2020) interpreted oceanic crust underlying the whole Falkland Plateau Basin. Although the seismic data presented here show folded Paleozoic deposits indicative of a more extensive continental crust in the east of the FIM than suggested by these studies, we do not refute the presence of oceanic crust

in the eastern part of the Falkland Plateau Basin. This would change the extent of the two sub-plates of the Falkland Plateau, but it would not affect the fact that the structural features of the Falkland Islands, North Falkland Basin, and the Volunteer and Fitzroy sub-basins are part of the same microplate and underwent the same amount of rotation. Therefore, we consider that the extent of the sub-plates and the overall crustal architecture of the plateau

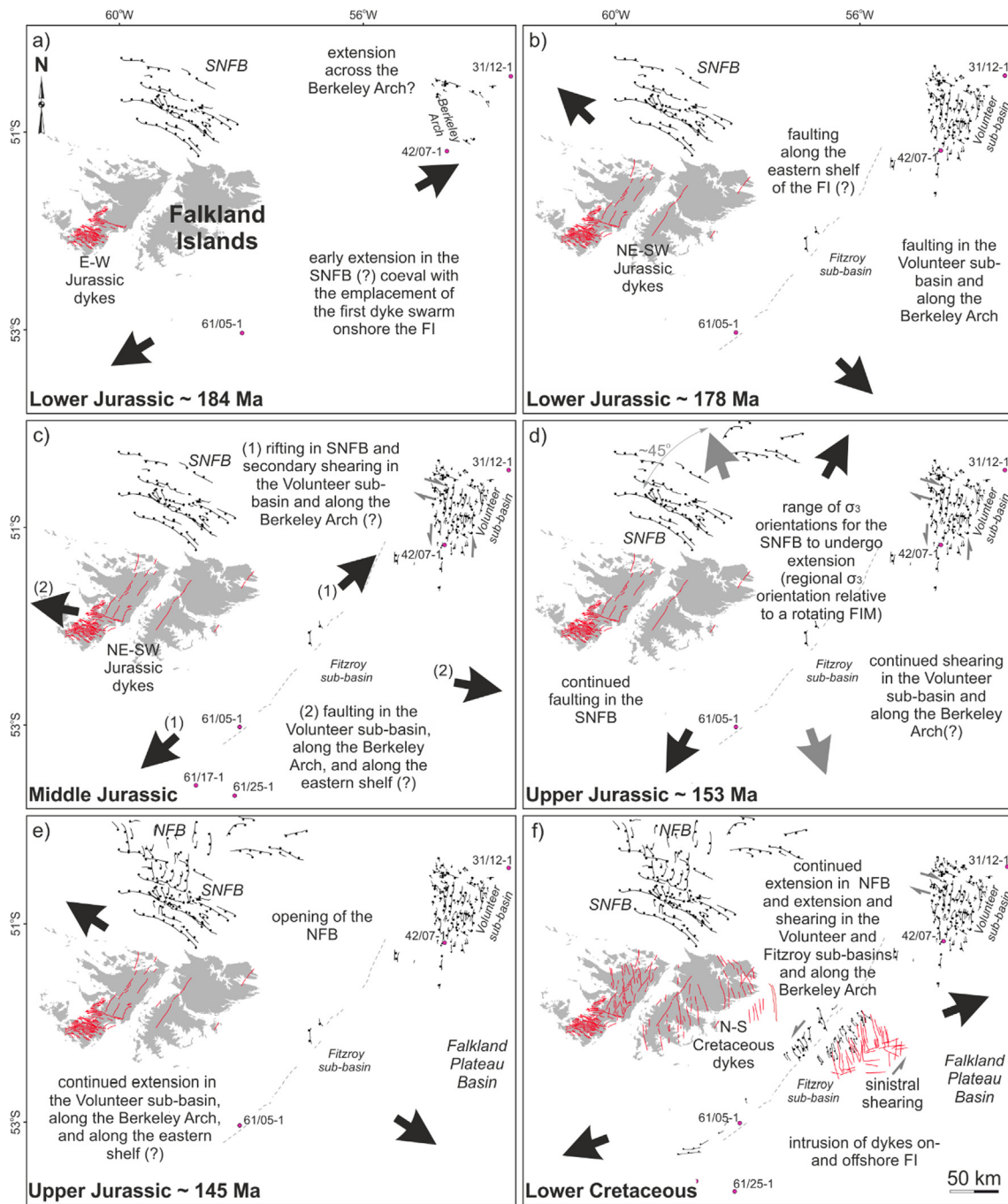


Fig. 16. Stress field evolution across the Falkland Islands Microplate (based on the structures from this study and literature, and the regional stress compilation in Fig. 15) throughout the Jurassic and Lower Cretaceous showing: a) Lower Jurassic emplacement of dykes onshore the islands and potential extension occurring in the Southern North Falkland Basin and across the Berkeley Arch; b) extension along the eastern shelf of the Falkland Islands and the emplacement of a NE-SW trending dyke swarm onshore; c) reactivation of the Southern North Falkland Basin faults and secondary shearing occurring in the Volunteer sub-basin area, followed by continued WNW-ESE directed extension in the Fitzroy and Volunteer sub-basins; d) reactivation of the faults in the Southern North Falkland Basin and continued shearing in the Volunteer sub-basin region; e) opening of the North Falkland Basin and extension along the eastern shelf of the Falkland Islands; f) Lower Cretaceous emplacement of dykes on- and offshore the Falkland Islands and continued extension and wrenching in the offshore basins; NFB – North Falkland Basin; SNFB – Southern North Falkland Basin; onshore and nearshore dykes drawn after Stone et al. (2009); SNFB and NFB fault networks after Lohr and Underhill (2015) and Stanca et al. (2019); no onshore structural features besides dykes are shown for simplicity (see Figs. 10 and 11 for the detailed map); arrows show extension direction and their orientation is equivalent to the orientation of σ_3 .

should not have implications for the purpose of this comparison between the local (FIM) and regional (south-western Gondwana) stresses. In the following section, the orientation of the regional σ_3 is mentioned relative to the fixed Africa (Fig. 15), whereas the local orientation is relative to the present-day position of the Falkland Islands (Fig. 16).

5.3.2. Local vs. regional stress orientation

The Lower Jurassic E-W trending dyke swarm onshore the Falkland Islands is thought to have compositional affinities with the now N-S trending Rooi Rand basalts in Lebombo, SE Africa (Armstrong et al. (1984) in Mitchell et al. (1999)), which were in turn correlated with the early E-W rifting between Africa and Antarctica (Reeves, 2000) (Fig. 15a). However, more recent dating

of the Rooi Rand dyke swarm yielded ages between 164.7 and 177.8 Ma (Jourdan et al., 2007; Hastie et al., 2014) and therefore younger than the Lower Jurassic dykes onshore the Falkland Islands (188 ± 2 to 190 ± 4 Ma). Older dyke swarms that mark the beginning of the Karoo-Ferrar magmatism and early stages of Gondwana fragmentation are the N-S striking dykes in the northern part of the Lebombo monocline in south-east Africa, although E-W regional extension might have started as early as 190 Ma with the emplacement of the ENE-WSW trending dykes from Ahlmannryggen region, Dronning Maud Land (Antarctica) (Riley et al., 2005; Jourdan et al., 2007; Klausen, 2009). The pre-break-up position of the Falkland Islands, incorporating the rotation from Stanca et al. (2019), would result in a NW-SE to N-S orientation of the oldest Jurassic dyke swarm relative to Africa. This is sub-parallel to the North Lebombo and the reconstructed Dronning Maud Land dykes, suggesting that their emplacement could have occurred in a similar stress regime (Fig. 15a). The Lower Jurassic dykes onshore the Falkland Islands show a more radial distribution (ENE-WSW swinging to WNW-ESE) which could suggest a continuation of their intrusion coeval with the Okavango and Save-Limpopo dyke swarms in Africa, discussed below, and a conjugate relationship with the NE-SW trending dykes onshore the Falkland Islands as suggested by Musset and Taylor (1994).

The Jurassic NE-SW (present-day orientation) oriented dyke swarm (162 ± 6 to 178.6 ± 4.9 Ma) has the same orientation as the Jurassic normal faults mapped along the Berkeley Arch and suggest a NW-SE to WNW-ESE orientation of σ_3 (Fig. 16b). The regional stress orientation during Lower Jurassic relative to a fixed Africa was controlled by NNW-SSE to N-S-oriented extension between East Antarctica and West Gondwana as inferred from field analysis of the Okavango and Save-Limpopo dyke swarms in Africa (Le Gall et al., 2002, 2005; Jourdan et al., 2007; Klausen, 2009; Hastie et al., 2014). At this time, NNW-SSE, NNE-SSW, and NE-SW striking dykes were emplaced in the Straumsvola, Ahlmannryggen, and Vestfjella regions, respectively, on the East Antarctic side (Riley et al., 2005; Curtis et al., 2008). The variation in the orientation of the Dronning Maud Land dyke swarms is considered to be suggestive of radial intrusions around a plume head (Curtis et al., 2008) rather than controlled by the regional stress field but are shown here in the interest of completeness. Rifting in the Weddell Sea Rift System (~ 175 – 180 Ma) and across Patagonia and the Malvinas Basin (Fig. 15a) is considered to have occurred during the Lower to Middle Jurassic (Jordan et al., 2017; Lovecchio et al., 2019; Riley et al., 2020), which is consistent with a roughly NNW-SSE regional extension relative to Africa. A counterclockwise rotation of the FIM to its original position would align the Lower to Upper Jurassic dykes perpendicular to the regional extension direction (Fig. 15a). However, the age range of these dykes is relatively wide and the age of the NE-SW trending normal faults along the Berkeley Arch is poorly constrained. These are speculated to be synchronous to the dyke emplacement based on their orientation alone. Faults and dykes with a similar trend would be generated during stage 2 of the Middle Jurassic extension (Fig. 15a) when the σ_3 rotates to an NNW-SSE orientation as East Antarctica drifts southwards (at ~ 167.2 Ma; König and Jokat, 2006). This would align the now WNW-ESE to NW-SE trending dykes of Middle Jurassic age (~ 170 Ma) from northern Patagonia (Rapalini and Lopez De Luchi, 2000; López De Luchi and Rapalini, 2002) with the Lower to Upper Jurassic dyke swarm from onshore the Falkland Islands and relate them to the same extensional episode (stage 2 of the Middle Jurassic deformation in Fig. 15a). This switch in the extension direction could also have led to the undocking of the FIM from Africa.

During the Upper Jurassic, the thrust faults in the SNFB undergo negative structural inversion and NW-SE to WNW-ESE trending normal faults are generated along the Berkeley Arch. These suggest

an NNW-SSE to NE-SW orientation of σ_3 (Fig. 16d). WSW-ENE directed extension is registered in the Outeniqua Basin (Paton and Underhill, 2004) related to the drifting of South America (Fig. 15a). This would require the FIM to be in an intermediary rotated position during the Upper Jurassic. The reactivated thrusts in the SNFB are in an orientation relative to the regional horizontal minimum stress that favours reactivation during the Lower and Middle Jurassic as well when E-W extension occurs between Africa and Antarctica (Fig. 15a) accompanied in the later stages by the emplacement of the Rooi Rand dykes (between 164.7 and 177.8 Ma; Jourdan et al., 2007) and the formation of the Northern Weddell Magnetic Province (~ 155 – 175 Ma; Grunow, 1993; Riley et al., 2020; Fig. 15a). This would point towards multiple phases of thrust reactivation in an extensional regime as suggested by the multiple synrift packages associated with them (Lohr and Underhill, 2015; Stanca et al., 2019). E-W trending faults (present-day orientation) documented by Stanca et al. (2019) north of the Falkland Islands would be generated synchronously to extension in the SNFB.

Little evidence for compression can be seen during this period (Fig. 13) in the north-eastern corner of the FIM (Volunteer sub-basin and Berkeley Arch). This could be due either to clockwise rotation against the Maurice Ewing Bank or related to the wrenching between eastern and western Gondwana or Africa and the Falkland Plateau. However, the small and localised scale of this compression suggests that the space into which the FIM rotated was in an overall extensional regime (i.e. the overall movement between Africa, South America, and Antarctica resulted in space being created at the same rate or faster than the FIM rotated, favouring the formation of predominantly extensional features over compressional or transpressional).

The Upper Jurassic to Lower Cretaceous normal faults in the NFB and Fitzroy sub-basin and the Lower Cretaceous (121 ± 1.2 Ma to 138 ± 4 Ma) on- and offshore dykes are consistent with a NE-SW regional extension direction (Paton and Underhill, 2004) related to the opening of the South Atlantic (Fig. 15b, c). This indicates that, at this stage, the FIM was roughly in its present-day position relative to South America (Fig. 15b, c).

Jurassic to Lower Cretaceous en-échélon normal faults in the Fitzroy sub-basin and along the Berkeley Arch suggest that some degree of sinistral wrenching occurred along the western NE-SW trending margin of the FPB during this time and WNW-ESE dextral shearing along the Berkeley Arch (Figs. 4, 14). This is consistent with intra-plate deformation related to a clockwise rotation of the FIM throughout the Jurassic. Further plate reorganization and/or wrenching related to movement on the AFFZ occur as late as Lower Cretaceous when evidence of WNW-ESE dextral shearing is identified along the Berkeley Arch and NE-SW sinistral wrenching is interpreted in the Fitzroy sub-basin (Figs. 4, 14). Large-scale NE-SW features (Fig. 4a, b and c) were identified further east on the plateau which we interpret as regional intra-plate sinistral shear zones that accommodated the rotation of the FIM with the small-scale en-échélon faults allowing further deformation along and between these features. Although geometries indicative of sinistral wrenching were identified on the seismic and gravity data (Figs. 4, 14), the amount of horizontal displacement along these potential fracture zones remains difficult to constrain.

Besides the NE-SW fault zones interpreted within the FPB, the Falkland Sound Fault, running between the West and East Falkland (Fig. 4a), follows the same trend and we could argue for a common origin. Studies carried along the Falkland Sound Fault suggest that these shear zones might be long-lived basement structures with activity recorded as early as late Paleozoic (Aldiss and Edwards, 1999; Stone, 2016) and re-established as left-lateral faults during the Mesozoic. However, based on the current data, the amount of displacement along these potential fracture zones cannot be quan-

tified. Dextral movement in the range of 3.3–300 km was interpreted along the Falkland Sound Fault during the Permo-Triassic or coeval with the break-up of Gondwana (Thomas et al., 1997; Curtis and Hyam, 1998; Aldiss and Edwards, 1999). However, no evidence of Jurassic or sinistral reactivation has been documented by more recent studies in the offshore sedimentary basins along-strike the Falkland Sound Fault (Richards et al., 1996; Lohr and Underhill, 2015; Stanca et al., 2019) which contributes to the uncertainty regarding the nature and age of this potential fracture zone. This precludes a correlation with the eastern fracture zones following the same trend and hinders a more detailed reconstruction of the microplate and an understanding of its overall geometry prior to the break-up.

5.3.3. Implications for the FIM rotation mechanism

Invoking the kinematic models of Ron et al. (1984), McKenzie and Jackson (1986), and Peacock et al. (1998) for the rotation of the FIM is a novel explanation. The extent of the blocks/microplates that have undergone this style of deformation related to large amounts of rotations in transform margin settings is sparsely documented. Examples of large recorded rotations, comparable to the FIM case, include the Santa Catalina Island (~90°) in South California (Luyendyk et al., 1985), albeit affecting a much smaller block (thousands versus hundreds of thousands of km²), and the Ellsworth-Whitmore Terrane (~90°) in Western Antarctica (comparable in areal extent to the FIM; Curtis and Storey, 1996). Instances where the deformation related to rotation was accommodated by strike-slip faults antithetic to the main shear zone (Ron et al., 1984; McKenzie and Jackson, 1986) are reported in the eastern and western Transverse Ranges in Southern California (Platt and Becker, 2013; Ingersoll and Coffey, 2017), and the oceanic Manus microplate (Bismarck Sea) in a back-arc spreading system (Martinez and Taylor, 1996). However, in none of these examples this style of deformation was both documented and led to >80° rotation of a microplate the size of the FIM.

We report evidence of sinistral wrenching across the FIM, potentially on several NE-SW striking shear zones (Fig. 4a, b and c). This observation is consistent with the kinematic models of Ron et al. (1984) and McKenzie and Jackson (1986), considering that the rotation of the FIM occurred in an overall dextral shear zone developed between East and West Gondwana, and Africa and South America. Furthermore, fault networks that are several orders of magnitude smaller, and suggestive of conjugate dextral and sinistral shearing have been interpreted along the eastern shelf of the Falkland Islands (Fig. 14). This is consistent with the model proposed by Peacock et al. (1998) where high degrees of block rotation can be accommodated through small-scale faulting and increased deformation within the block itself (Fig. 4a, d and Fig. 14). Although these models can be used to interpret the current structural architecture of the FIM, more data is required to constrain whether the microplate rotated as a whole, or whether the NE-SW shear zones are responsible for a further fragmentation of the FIM. Furthermore, the answer to why this particular transform margin has seen such high degrees of rotation affecting a microplate several hundred of kilometers wide remains elusive. Possibly this is a consequence of the origin of the microplate at a junction of multiple tectonic plates, where rapid variations in the stress configuration are expected, followed by its evolution along one of the most long-lived and long-offset transform faults on Earth. Alternatively, it is the result of deeper processes that preconditioned this scale of rotation, and ultimately led to the break-up of Gondwana (Ben-Avraham et al., 1993; Storey, 1995; Dalziel et al., 2000). Nonetheless, we advocate testing the kinematic models of Ron et al. (1984), McKenzie and Jackson (1986), and Peacock et al. (1998) in other settings where comparable scales of micro-

plates and amount of rotation require a mechanistic explanation (e.g. the Ellsworth Whitmore Terrane).

6. Conclusions

The western margin of the Falkland Plateau Basin recorded a series of rapid changes in the orientation of σ_3 during the Jurassic and Lower Cretaceous related to a vertical-axis rotation of the Falkland Islands Microplate. This rotation took place under a complex stress regime corresponding to the region located between South America, Africa, and East Antarctica and the early stages of transform margin formation.

The clockwise rotation resulted in the generation of NE-SW and WNW-ESE trending faults in the northern part of the margin (along the Berkeley Arch and in the Volunteer sub-basin) superimposed by N-S striking en-*é*chelon normal faults extending into the Fitzroy sub-basin. When collated with information from the North Falkland Basin and onshore the Falkland Islands, the larger structural framework supports a complex tectonic history of the FIM. The orientation of the minimum horizontal stress across the FIM alternated between roughly NE-SW and NW-SE/WWN-ESE during the Jurassic and switched to a NE-SW orientation during the Lower Cretaceous.

Interpretation of seismic reflection data along the eastern shelf of the FIM points towards a larger eastern extent of the microplate than previously constrained. The revised microplate comprises the region of the Volunteer and Fitzroy sub-basins. A comparison of the newly defined FIM local stress configuration with the regional stress in the reconstructed south-western Gondwana suggests that the rotation of the microplate started during or after the intrusion of the Jurassic NE-SW trending dykes onshore the Falkland Islands (during the drift initiation of East Antarctica in Middle Jurassic) and continued throughout the Upper Jurassic. During the incipient stages of rotation, a small degree of compression occurred in the north-eastern corner of the microplate, but the predominant extensional structures suggest that the early fragmentation of Gondwana generated enough space during the clockwise rotation of the islands to limit the widespread occurrence of compression.

CRediT authorship contribution statement

Roxana M. Stanca: Conceptualization, Methodology, Validation, Formal analysis, Investigation, Writing – original draft, Visualization. **Dave J. McCarthy:** Conceptualization, Resources, Writing – review & editing, Visualization – review & editing, Supervision, Funding acquisition. **Douglas A. Paton:** Conceptualization, Methodology, Resources, Supervision, Funding acquisition. **David M. Hodgson:** Conceptualization, Writing – review & editing, Visualization – review & editing, Supervision, Funding acquisition. **Estelle J. Mortimer:** Conceptualization, Writing – review & editing, Visualization – review & editing, Supervision, Funding acquisition.

Declaration of Competing Interest

The authors declare that they have no known competing financial interests or personal relationships that could have appeared to influence the work reported in this paper.

Acknowledgements

We thank Graham Leslie (British Geological Survey) for the thorough in-house review. Gondwana Research's Associate Editor, Nicholas Rawlinson, and the journal's reviewer, Graeme Eagles, are thanked for the constructive comments on our original manuscript. This paper is published by permission of the Director of Mineral

Resources, Falkland Islands Government, and the Executive Director, British Geological Survey (BGS). The work in this paper is part of a Leeds/York NERC Doctoral Training Programme and BGS-funded project.

References

- Adie, R.J., 1952. The Position of the Falkland Islands in a Reconstruction of Gondwanaland. *Geol. Mag.* 89 (06), 401. <https://doi.org/10.1017/S0016756800068102>.
- Aldiss, D.T., Edwards, E.J., 1999. The geology of the Falkland Islands. British Geological Survey Technical Report WC/99/10. Available at: <http://nora.nerc.ac.uk/507542/>.
- Armstrong, R.A., Bristow, J.W., Cox, K.G., 1984. The Rooi Rand dyke swarm, southern Lebombo. In: Erlank, A.J. (Ed.) *Petrogenesis of the volcanic rocks of the Karoo province*. *Spec. Publ. Geol. Soc. S. Afr.*, 13, pp. 77–86.
- Baby, G., Guillocheau, F., Boulogne, C., Robin, C., Dall'Asta, M., 2018. Uplift history of a transform continental margin revealed by the stratigraphic record: The case of the Agulhas transform margin along the Southern African Plateau DOME. *Tectonophysics* 731–732, 104–130. <https://doi.org/10.1016/j.tecto.2018.03.014>.
- Baristean, N., Anka, Z., di Primio, R., Rodriguez, J.F., Marchal, D., Dominguez, F., 2013. New insights into the tectono-stratigraphic evolution of the Malvinas Basin, offshore of the southernmost Argentinean continental margin. *Tectonophysics* 604, 280–295. <https://doi.org/10.1016/j.tecto.2013.06.009>.
- Barker, P.F., 1977. Correlations between Sites on the Eastern Falkland Plateau by Means of Seismic Reflection Profiles, Leg 36, DSDP. Initial Reports of the Deep Sea Drilling Project 36. <https://doi.org/10.2973/dsdp.proc.36.128.1977>.
- Barker, P.F., Dalziel, I.W.D., Dinkelmann, M.G., Elliot, D.H., Gombos, A.M., Jr., Lonardi, A., Plafker, G., Tarney, J., Thompson, R.W., Tjalsma, R.C., von der Borch, C.C., Wise, S.W., Jr., Harris, W.K., Sliter, W.V., 1977. Site 330. Texas A & M University, Ocean Drilling Program, College Station, TX, United States. doi:10.2973/dsdp.proc.36.106.1977.
- Barker, P.F., 1999. Evidence for a volcanic rifted margin and oceanic crustal structure for the Falkland Plateau Basin. *J. Geol. Soc. London* 156 (5), 889–900. <https://doi.org/10.1144/gsjgs.156.5.0889>.
- Ben-Avraham, Z., Hartnady, C.J.H., Malan, J.A., 1993. Early tectonic extension between the Agulhas Bank and the Falkland Plateau due to the rotation of the Lafonia microplate. *Earth Planet. Sci. Lett.* 117 (1–2), 43–58. [https://doi.org/10.1016/0012-821X\(93\)90116-Q](https://doi.org/10.1016/0012-821X(93)90116-Q).
- Del Ben, A., Mallardi, A., 2004. Interpretation and chronostratigraphic mapping of multichannel seismic reflection profile I95167, Eastern Falkland Plateau (South Atlantic). *Mar. Geol.* 209 (1–4), 347–361. <https://doi.org/10.1016/j.margeo.2004.06.008>.
- BHP Billiton Petroleum, 2010. Well completion report, Toroa-1, FI 61/05-1. Unpublished.
- Bouhier, V.E., Franchini, M.B., Caffè, P.J., Maydagán, L., Rapela, C.W., Paolini, M., 2017. Petrogenesis of volcanic rocks that host the world-class Ag–Pb Navidad District, North Patagonian Massif: Comparison with the Jurassic Chon Aike Volcanic Province of Patagonia, Argentina. *J. Volcanol. Geotherm. Res.* 338, 101–120. <https://doi.org/10.1016/j.jvolgeores.2017.03.016>.
- Bry, M., White, N., Singh, S., England, R., Trowell, C., 2004. Anatomy and formation of oblique continental collision: South Falkland basin. *Tectonics* 23 (4), 1–20. <https://doi.org/10.1029/2002TC001482>.
- Chemale, F., Ramos, V.A., Naipauer, M., Girelli, T.J., Vargas, M., 2018. Age of basement rocks from the Maurice Ewing Bank and the Falkland/Malvinas Plateau. *Precambrian Res.* 314, 28–40. <https://doi.org/10.1016/j.precamres.2018.05.026>.
- Cordell, L., Grauch, V.J.S., 1985. Mapping basement magnetization zones from aeromagnetic data in the San Juan Basin, New Mexico. In: Hinz, W.J. (Ed.), *The Utility of Regional Gravity and Magnetic Anomaly Maps*. Society of Exploration Geophysicists, Tulsa, OK, pp. 181–197.
- Covault, J.A., 2011. Submarine fans and canyon-channel systems: a review of processes, products, and models. *Nature Educ. Knowl.* 3 (10).
- Cunningham, A.P., Barker, P.F., Tomlinson, J.S., 1998. Tectonics and sedimentary environment of the North Scotia Ridge region revealed by side-scan sonar. *J. Geol. Soc. London* 155 (6), 941–956. <https://doi.org/10.1144/gsjgs.155.6.0941>.
- Curtis, M.L., Riley, T.R., Owens, W.H., Leat, P.T., Duncan, R.A., 2008. The form, distribution and anisotropy of magnetic susceptibility of Jurassic dykes in H.U. Sverdrupfjella, Dronning Maud Land, Antarctica. Implications for dyke swarm emplacement. *J. Struct. Geol.* 30 (11), 1429–1447. <https://doi.org/10.1016/j.jsg.2008.08.004>.
- Curtis, M.L., Hyam, D.M., 1998. Late Palaeozoic to Mesozoic structural evolution of the Falkland Islands: a displaced segment of the Cape Fold Belt. *J. Geol. Soc. London* 155 (1), 115–129. <https://doi.org/10.1144/gsjgs.155.1.0115>.
- Curtis, M.L., Storey, B.C., 1996. A review of geological constraints on the pre-break-up position of the Ellsworth Mountains within Gondwana: implications for Weddell Sea evolution. *Geol. Soc. Spec. Publ.* 108 (1), 11–30. <https://doi.org/10.1144/GSL.SP.1996.108.01.02>.
- Dalziel, I.W.D., Lawver, L.A., Murphy, J.B., 2000. Plumes, orogenesis, and supercontinental fragmentation. *Earth Planet. Sci. Lett.* 178 (1–2), 1–11. [https://doi.org/10.1016/S0012-821X\(00\)00061-3](https://doi.org/10.1016/S0012-821X(00)00061-3).
- Dodd, T.J.H., McCarthy, D.J., 2016. The Berkley Arch: Seaward Dipping Reflectors or a missing slice of the Cape Fold Thrust Belt?. In: *The Roberts Conference Passive Margins*. 10.13140/RG.2.2.13836.97928.
- Eagles, G., Eisermann, H., 2020. The Skytrain plate and tectonic evolution of southwest Gondwana since Jurassic times. *Sci. Rep. Nature Publishing Group UK* 10 (1), 1–17. <https://doi.org/10.1038/s41598-020-77070-6>.
- Eagles, G., Vaughan, A.P.M., 2009. Gondwana breakup and plate kinematics: business as usual. *Geophys. Res. Lett.* 36 (10), 2–5. <https://doi.org/10.1029/2009GL037552>.
- Eagles, G., 2000. Modelling plate kinematics in the Scotia Sea Ph.D. Thesis. University of Leeds.
- Elliot, D.H., 1992. Jurassic magmatism and tectonism associated with Gondwanaland break-up: an Antarctic perspective. *Geol. Soc. Spec. Publ.* 68 (68), 165–184. <https://doi.org/10.1144/GSL.SP.1992.068.01.11>.
- Elliot, D.H., Fleming, T.H., Kyle, P.R., Folland, K.A., 1999. Long-distance transport of magmas in the Jurassic Ferrar Large Igneous Province, Antarctica. *Earth Planet. Sci. Lett.* 167 (1–2), 89–104. [https://doi.org/10.1016/S0012-821X\(99\)00023-0](https://doi.org/10.1016/S0012-821X(99)00023-0).
- Encarnación, J., Fleming, T.H., Elliot, D.H., Eales, H.V., 1996. Synchronous emplacement of Ferrar and Karoo dolerites and the early breakup of Gondwana. *Geology* 24 (6), 535–538. [https://doi.org/10.1130/0091-7613\(1996\)024<0535:SEOFAK>2.3.CO;2](https://doi.org/10.1130/0091-7613(1996)024<0535:SEOFAK>2.3.CO;2).
- Ewing, J.I., Ludwig, W.J., Ewing, M., Eittrheim, S.L., 1971. Structure of the Scotia Sea and Falkland Plateau. *J. Geophys. Res.* 76 (29), 7118–7137.
- Falkland Oil and Gas Limited, 2013. Geological well completion report, Scotia East D, FI 31/12-1. Unpublished.
- Franzese, J., Martino, R., 1998. Aspectos cinemáticos y tectónicos de la zona de cizalla de Gastre en la sierra de Calcatapul, provincia de Chubut, Argentina. In: 10° Congreso Latinoamericano de Geología y 6° Congreso Nacional de Geología Económica, 2, pp. 3.
- GEBCO Compilation Group, 2020. GEBCO 2020 Grid. doi:10.5285/a29c5465-b138-234d-e053-6c86abc040b9.
- Gomez, S.C., 2001. A catalogue of dykes from aeromagnetic surveys in eastern and southern Africa. Enschede: The International Institute for Aerospace Survey and Earth Sciences (ITC).
- Grunow, A.M., 1993. New paleomagnetic data from the Antarctic Peninsula and their tectonic implications. *J. Geophys. Res.* 98 (B8), 13815–13833. <https://doi.org/10.1029/93JB01089>.
- Hastie, W.W., Watkeys, M.K., Aubourg, C., 2014. Magma flow in dyke swarms of the Karoo LIP: implications for the mantle plume hypothesis. *Gondwana Res.* 25 (2), 736–755. <https://doi.org/10.1016/j.gr.2013.08.010>.
- Heine, C., Zoethout, J., Müller, R.D., 2013. Kinematics of the South Atlantic rift. *Solid Earth* 4 (2), 215–253. <https://doi.org/10.5194/se-4-215-2013>.
- Henza, A.A., Withjack, M.O., Schlische, R.W., 2010. Normal-fault development during two phases of non-coaxial extension: an experimental study. *J. Struct. Geol.* 32 (11), 1656–1667. <https://doi.org/10.1016/j.jsg.2009.07.007>.
- Hodgkinson, R., 2002. Structural studies in the Falkland Islands, South Atlantic Unpublished PhD Thesis. University of Birmingham, UK.
- Hole, M.J., Ellam, R.M., Macdonald, D.I.M., Kelley, S.P., 2016. Gondwana break-up related magmatism in the Falkland Islands. *J. Geol. Soc.* 173 (1), 108–126. <https://doi.org/10.1144/jgs2015-027>.
- Hubbard, R.J., Pape, J., Roberts, D.G., 1985a. Depositional sequence mapping as a technique to establish tectonic and stratigraphic framework and evaluate hydrocarbon potential on a passive continental margin. In: Berg, O.R., Woolverton, D. (Eds.) *Seismic Stratigraphy II: An Integrated Approach to Hydrocarbon Exploration*. AAPG Memoirs, 39, pp. 79–91.
- Hubbard, R.J., Pape, J., Roberts, D.G., 1985b. Depositional sequence mapping to illustrate the evolution of a passive continental margin. In: Berg, O.R., Woolverton, D. (Eds.) *Seismic Stratigraphy II: An Integrated Approach to Hydrocarbon Exploration*. AAPG Memoirs, 39, pp. 93–115.
- Ingersoll, R.V., Coffey, K.T., 2017. Transrotation induced by crustal blocks moving through restraining double bends, with Southern California Examples. *J. Geol.* 125 (5), 551–559. <https://doi.org/10.1086/692654>.
- Jacobs, J., Thomas, R.J., Armstrong, R.A., Henjes-Kunst, F., 1999. Age and thermal evolution of the Mesoproterozoic Cape Meredith Complex, West Falkland. *J. Geol. Soc.* 156 (5), 917–928. <https://doi.org/10.1144/gsjgs.156.5.0917>.
- Jacobs, J., Bauer, W., Fanning, C.M., 2003. Late Neoproterozoic/Early Palaeozoic events in central Dronning Maud Land and significance for the southern extension of the East African Orogen into East Antarctica. *Precambrian Res.* 126 (1–2), 27–53. [https://doi.org/10.1016/S0301-9268\(03\)00125-6](https://doi.org/10.1016/S0301-9268(03)00125-6).
- Jacobs, J., Thomas, R.J., 2004. Himalayan-type indenter-escape tectonics model for the southern part of the late Neoproterozoic-early Paleozoic East African-Antarctic orogen. *Geology* 32 (8), 721–724. <https://doi.org/10.1130/G20516.1>.
- Jordan, T.A., Ferraccioli, F., Leat, P.T., 2017. New geophysical compilations link crustal block motion to Jurassic extension and strike-slip faulting in the Weddell Sea Rift System of West Antarctica. *Gondwana Res.* 42, 29–48. <https://doi.org/10.1016/j.jgr.2016.09.009>.
- Jourdan, F., Féraud, G., Bertrand, H., Watkeys, M.K., 2007. From flood basalts to the inception of oceanization: Example from the ⁴⁰Ar/³⁹Ar high-resolution picture of the Karoo large igneous province. *Geochem. Geophys. Geosyst.* 8 (2). <https://doi.org/10.1029/2006GC001392>.
- Kimbell, G.S., Richards, P.C., 2008. The three-dimensional lithospheric structure of the Falkland Plateau region based on gravity modelling. *J. Geol. Soc. London* 165 (4), 795–806. <https://doi.org/10.1144/0016-76492007-114>.
- Klausen, M.B., 2009. The Lebombo monocline and associated feeder dyke swarm: diagnostic of a successful and highly volcanic rifted margin? *Tectonophysics* 468 (1–4), 42–62. <https://doi.org/10.1016/j.tecto.2008.10.012>.

- König, M., Jokat, W., 2006. The Mesozoic breakup of the Weddell Sea. *J. Geophys. Res. Solid Earth* 111 (12), 1–28. <https://doi.org/10.1029/2006JB004035>.
- Lawrence, S.R., Johnson, M., Tubb, S.R., Marshallsea, S.J., 1999. Tectono-stratigraphic evolution of the North Falkland region. *Geol. Soc. Spec. Publ.* 153 (1), 409–424. <https://doi.org/10.1144/GSL.SP.1999.153.01.25>.
- Lawver, L.A., Gahagan, L.M., Dalziel, I.W.D., 1999. A tight fit - Early Mesozoic Gondwana, a plate reconstruction perspective. *Mem. Natl. Inst. Polar Res. Special Issue* 53, 214–229.
- Le Gall, B., Tshoso, G., Jourdan, F., Féraud, G., Bertrand, H., Tiercelin, J.J., Kampunzu, A.B., Modisi, M.P., Dymont, J., Maia, M., 2002. $^{40}\text{Ar}/^{39}\text{Ar}$ geochronology and structural data from the giant Okavango and related mafic dyke swarms, Karoo Igneous province, Northern Botswana. *Earth Planet. Sci. Lett.* 202 (3–4), 595–606. [https://doi.org/10.1016/S0012-821X\(02\)00763-X](https://doi.org/10.1016/S0012-821X(02)00763-X).
- Le Gall, B., Tshoso, G., Dymont, J., Kampunzu, A.B., Jourdan, F., Féraud, G., Bertrand, H., Aubourg, C., Vétel, W., 2005. The Okavango giant mafic dyke swarm (NE Botswana): Its structural significance within the Karoo Large Igneous Province. *J. Struct. Geol.* 27 (12), 2234–2255. <https://doi.org/10.1016/j.jsg.2005.07.004>.
- Lohr, T., Underhill, J.R., 2015. Role of rift transection and punctuated subsidence in the development of the North Falkland Basin. *Pet. Geosci.* 21 (2–3), 85–110. <https://doi.org/10.1144/petgeo2014-050>.
- López De Luchi, M.G., Rapalini, A.E., 2002. Middle Jurassic dyke swarms in the North Patagonian Massif: The Lonco trap formation in the Sierra de Mamil Choique, Río Negro province, Argentina. *J. S. Am. Earth Sci.* 15 (6), 625–641. [https://doi.org/10.1016/S0895-9811\(02\)00083-4](https://doi.org/10.1016/S0895-9811(02)00083-4).
- Lorenzo, J.M., Mutter, J.C., 1988. Seismic stratigraphy and tectonic evolution of the Falkland/Malvinas Plateau. *Braz. J. Geol.* 18 (2), 11p.
- Lovecchio, J.P., Naipauer, M., Cayo, L.E., Rohais, S., Giunta, D., Flores, G., Gerster, R., Bolatti, N.D., Joseph, P., Valencia, V.A., Ramos, V.A., 2019. Rifting evolution of the Malvinas basin, offshore Argentina: New constraints from zircon U-Pb geochronology and seismic characterization. *J. S. Am. Earth Sci.* 95, 102253. <https://doi.org/10.1016/j.jsames.2019.102253>.
- Ludwig, W.J., Krashennnikov, V.A., Basov, I.A., Bayer, U., Bloemendal, J., Bornhold, B., Ciesielski, P., Goldstein, E.H., Robert, C., Salloway, J.C., Usher, J.L., von der Dick, H., Weaver, F.M., Wise, S.W., 1980. Site 512. Initial Reports of the Deep Sea Drilling Project, Volume 71.
- Ludwig, W.J., Krashennnikov, V.A., Basov, I.A., Bayer, U., Bloemendal, J., Bornhold, B., Ciesielski, P., Goldstein, E.H., Robert, C., Salloway, J.C., Usher, J.L., von der Dick, H., Weaver, F.M., Wise, S.W., 1983. Site 511. Initial Reports of the Deep Sea Drilling Project, Volume 71, pp. 21–109. doi:10.2973/dsdp.proc.71.102.1983.
- Ludwig, W.J., Windisch, C.C., Houtz, R.E., Ewing, J.L., 1978. Structure of Falkland Plateau and Offshore Tierra del Fuego, Argentina. *Am. Assoc. Pet. Geol. Memoir* 29, 125–137.
- Ludwig, W.J., 1983. Geologic Framework of the Falkland Plateau. Initial Reports of the Deep Sea Drilling Project 71, 281–293. <https://doi.org/10.2973/dsdp.proc.71.107.1983>.
- Luyendyk, B.P. et al., 1985. Simple shear of southern California during Neogene time suggested by paleomagnetic declinations (USA). *J. Geophys. Res.* 90 (B14), 454–466. <https://doi.org/10.1029/jb090ib14p12454>.
- Macdonald, D., Gomez-Perez, I., Franzese, J., Spalletti, L., Lawver, L., Gahagan, L., Dalziel, I., Thomas, C., Trewin, N., Hole, M., Paton, D., 2003. Mesozoic break-up of SW Gondwana: implications for regional hydrocarbon potential of the southern South Atlantic. *Mar. Pet. Geol.* 20 (3–4), 287–308. [https://doi.org/10.1016/S0264-8172\(03\)00045-X](https://doi.org/10.1016/S0264-8172(03)00045-X).
- Magee, C., Jackson, C.A., 2019. [Pre-print] How do normal faults grow above dykes? 10.31223/osf.io/ahxn5.
- Marshall, J.E.A., 1994. The Falkland Islands: A key element in Gondwana paleogeography. *Tectonics* 13 (2), 499–514.
- Martin, A.K., Hartnady, C.J.H., Goodlad, S.W., 1981. A revised fit of South America and South Central Africa. *Earth Planet. Sci. Lett.* 54 (2), 293–305. [https://doi.org/10.1016/0012-821X\(81\)90012-1](https://doi.org/10.1016/0012-821X(81)90012-1).
- Martinez, F., Taylor, B., 1996. Backarc spreading, rifting, and microplate rotation, between transform faults in the Manus Basin. *Mar. Geophys. Res.* 18 (2–4), 203–224. <https://doi.org/10.1007/BF00286078>.
- Masclé, J., Mougénot, D., Blarez, E., Marinho, M., Virlogeux, P., 1987. African transform continental margins: Examples from Guinea, the Ivory Coast and Mozambique. *Geol. J.* 22 (S2), 537–561. [https://doi.org/10.1002/\(ISSN\)1099-103410.1002/gj.v22:2+10.1002/gj.3350220632](https://doi.org/10.1002/(ISSN)1099-103410.1002/gj.v22:2+10.1002/gj.3350220632).
- McKenzie, D., Jackson, J., 1986. A block model of distributed deformation by faulting. *J. Geol. Soc. London* 143 (2), 349–353. <https://doi.org/10.1144/gsjgs.143.2.0349>.
- McMillan, I.K., 2003. Foraminiferally defined biostratigraphic episodes and sedimentation pattern of the Cretaceous drift succession (Early Barremian to Late Maastrichtian) in seven basins on the South African and southern Namibian continental margin. *S. Afr. J. Sci.* 99 (11–12), 537–576.
- Miller, H.G., Singh, V., 1994. Potential field tilt - A new concept for location of potential field sources. *J. Appl. Geophys.* 32 (2–3), 213–217. [https://doi.org/10.1016/0926-9851\(94\)90022-1](https://doi.org/10.1016/0926-9851(94)90022-1).
- Mitchell, C., Taylor, G.K., Cox, K.G., Shaw, J., 1986. Are the Falkland Islands a rotated microplate? *Nature* 319 (6049), 131–134. <https://doi.org/10.1038/319131a0>.
- Mitchell, C., Ellam, R.M., Cox, K.G., 1999. Mesozoic dolerite dykes of the Falkland Islands: petrology, petrogenesis and implications for geochemical provinciality in Gondwanaland low-Ti basaltic rocks. *J. Geol. Soc. London* 156 (5), 901–916. <https://doi.org/10.1144/gsjgs.156.5.901>.
- Mitchum, R.M., Jr., Vail, P.R., Sangree, J.B., 1977. Seismic stratigraphy and global changes of sea level; part 6, stratigraphic interpretation of seismic reflection patterns in depositional sequences. In: Payton, C.E. (Ed.) *Seismic Stratigraphy: Applications to Hydrocarbon Exploration*. AAPG Memoirs, 26, pp. 117–134.
- Müller, R.D., Zahirovic, S., Williams, S.E., Cannon, J., Seton, M., Bower, D.J., Tetley, M., Heine, C., Le Breton, E., Liu, S., Russell, S.H.J., Yang, T., Leonard, J., Gurnis, M., 2019. A global plate model including lithospheric deformation along major rifts and orogens since the Triassic. *Tectonics* 38 (6), 1884–1907. <https://doi.org/10.1029/2018TC005462>.
- Mussett, A.E., Taylor, G.K., 1994. ^{40}Ar - ^{39}Ar ages for dykes from the Falkland Islands with implications for the break-up of southern Gondwanaland. *J. Geol. Soc. London* 151 (1), 79–81. <https://doi.org/10.1144/gsjgs.151.1.0079>.
- Nemčok, M., Sinha, S.T., Doré, A.G., Lundin, E.R., Mascle, J., Rybár, S., 2016. Mechanisms of microcontinent release associated with wrenching-involved continental break-up; a review. *Geol. Soc. Spec. Publ.* 431, 323–359. <https://doi.org/10.1144/SP431.14>.
- Orcu, B., Keskinsezer, A., 2008. Structural setting of the northeastern Biga Peninsula (Turkey) from tilt derivatives of gravity gradient tensors and magnitude of horizontal gravity components. *Pure Appl. Geophys.* 165 (9–10), 1913–1927. <https://doi.org/10.1007/s00024-008-0407-8>.
- Parsieglä, N., Stankiewicz, J., Gohl, K., Ryberg, T., Uenzelmann-Neben, G., 2009. Southern African continental margin: dynamic processes of a transform margin. *Geochim. Geophys. Geosyst.* 10 (3), n/a–n/a. <https://doi.org/10.1029/2008GC002196>.
- Paton, D.A., Underhill, J.R., 2004. Role of crustal anisotropy in modifying the structural and sedimentological evolution of extensional basins: the Gamtoos Basin, South Africa. *Basin Res.* 16 (3), 339–359. <https://doi.org/10.1111/j.1365-2117.2004.00237.x>.
- Paton, D.A., Macdonald, D.I.M., Underhill, J.R., 2006. Applicability of thin or thick skinned structural models in a region of multiple inversion episodes; southern South Africa. *J. Struct. Geol.* 28 (11), 1933–1947. <https://doi.org/10.1016/j.jsg.2006.07.002>.
- Peacock, D.C.P., Anderson, M.W., Morris, A., Randall, D.E., 1998. Evidence for the importance of “small” faults on block rotation. *Tectonophysics* 299 (1–3), 1–13.
- Platt, J.P., Becker, T.W., 2013. Kinematics of rotating panels of E-W faults in the san andreas system: What can we tell from geodesy? *Geophys. J. Int.* 194 (3), 1295–1301. <https://doi.org/10.1093/gji/ggt189>.
- Platt, N.H., Philip, P.R., 1995. Structure of the southern Falkland Islands continental shelf: initial results from new seismic data. *Mar. Pet. Geol.* 12 (7), 759–771. [https://doi.org/10.1016/0264-8172\(95\)93600-9](https://doi.org/10.1016/0264-8172(95)93600-9).
- Rabinowitz, P.D., Labrecque, J., 1979. The Mesozoic South Atlantic Ocean and evolution of its continental margins. *J. Geophys. Res.* 84 (B11), 5973–6002. <https://doi.org/10.1029/JB084iB11p05973>.
- Ramos, V.A., 2008. Patagonia: A paleozoic continent adrift? *J. S. Am. Earth Sci.* 26 (3), 235–251. <https://doi.org/10.1016/j.jsames.2008.06.002>.
- Ramos, V.A., Cingolani, C., Junior, F.C., Naipauer, M., Rapalini, A., 2017. The Malvinas (Falkland) Islands revisited: The tectonic evolution of southern Gondwana based on U-Pb and Lu-Hf detrital zircon isotopes in the Paleozoic cover. *J. S. Am. Earth Sci.* 76, 320–345. <https://doi.org/10.1016/j.jsames.2016.12.013>.
- Rapalini, A.E., Lopez De Luchi, M., 2000. Paleomagnetism and magnetic fabric of Middle Jurassic dykes from Western Patagonia, Argentina. *Phys. Earth Planet. Inter.* 120 (1), 11–27. [https://doi.org/10.1016/S0031-9201\(00\)00140-0](https://doi.org/10.1016/S0031-9201(00)00140-0).
- Rapela, C.W., Pankhurst, R.J., 1992. The granites of northern Patagonia and the Gastre Fault System in relation to the break-up of Gondwana. *Geol. Soc. Spec. Publ.* 68 (1), 209–220. <https://doi.org/10.1144/GSL.SP.1992.068.01.13>.
- Reeves, C., 2000. The geophysical mapping of Mesozoic dyke swarms in southern Africa and their origin in the disruption of Gondwana. *J. African Earth Sci.* 30 (3), 499–513.
- Richards, P.C., Gatloff, R.W., Quinn, M.F., Williamson, J.P., Fannin, N.G.T., 1996. The geological evolution of the Falkland Islands continental shelf. In: Storey, B.C., King, E.C., Livermore, R.A., (Eds.), *Weddell Sea Tectonics and Gondwana Break-up*. *Geol. Soc. Spec. Publ.*, 108, pp. 105–128. <https://doi.org/10.1144/GSL.SP.1996.108.01.08>.
- Richards, P.C., Stone, P., Kimbrell, G.S., McIntosh, W.C., Phillips, E.R., 2013. Mesozoic magmatism in the Falkland Islands (South Atlantic) and their offshore sedimentary basins. *J. Pet. Geol.* 36 (1), 61–73. <https://doi.org/10.1111/jpg.12542>.
- Richards, P.C., Fannin, N.G.T., 1997. Geology of the North Falkland Basin. *J. Pet. Geol.* 20 (2), 165–183. <https://doi.org/10.1111/jpg.1997.20.issue-210.1111/j.1747-5457.1997.tb00771.x>.
- Riley, T.R., Leat, P.T., Curtis, M.L., Millar, I.L., Duncan, R.A., Fazel, A., 2005. Early - Middle Jurassic dolerite dykes from Western Dronning Maud Land (Antarctica): identifying mantle sources in the Karoo Large Igneous Province. *J. Pet. Geol.* 46 (7), 1489–1524. <https://doi.org/10.1093/petrology/egi023>.
- Riley, T.R., Jordan, T.A.R.M., Leat, P.T., Curtis, M.L., Millar, I.L., 2020. Magmatism of the Weddell Sea rift system in Antarctica: Implications for the age and mechanism of rifting and early stage Gondwana breakup. *Gondwana Res.* 79, 185–196. <https://doi.org/10.1016/j.gr.2019.09.014>.
- Rockhopper Exploration Plc., 2012. [In-house presentation] The East Falklands Basin. Available at: <http://www7.investorrelations.co.uk/fog/uploads/companypresentations/TheEastFalklandsBasin-2012DrillingProgramme.pdf>.
- Ron, H., Freund, R., Garfunkel, Z., Nur, A., 1984. Block rotation by strike-slip faulting: structural and paleomagnetic evidence. *J. Geophys. Res.* 89 (B7), 6256–6270.
- Sandwell, D.T., Müller, R.D., Smith, W.H.F., Garcia, E., Francis, R., 2014. New global marine gravity model from CryoSat-2 and Jason-1 reveals buried tectonic structure. *Science* 346 (6205). <https://doi.org/10.1126/science.1258213>.

- Schimschal, C.M., Jokat, W., 2017. The crustal structure of the continental margin east of the Falkland Islands. *Tectonophysics*. Elsevier B.V. <https://doi.org/10.1016/j.tecto.2017.11.034>.
- Schimschal, C.M., Jokat, W., 2019. The Falkland Plateau in the context of Gondwana breakup. *Gondwana Res.* 68, 108–115. <https://doi.org/10.1016/j.gr.2018.11.011>.
- Schreider, A.A., Mazo, E.L., Bulychev, A.A., Schreider, A.A., Gilod, D.A., Kulikova, M.P., 2011. The structure of the Falkland Basin's lithosphere. *Oceanology* 51 (5), 866–875. <https://doi.org/10.1134/S0001437011050171>.
- Scrutton, R.A., 1979. On sheared passive continental margins. *Tectonophysics* 59 (1–4), 293–305.
- Stanca, R.M., Paton, D.A., Hodgson, D.M., McCarthy, D.J., Mortimer, E.J., 2019. A revised position for the rotated Falkland Islands microplate. *J. Geol. Soc. London* 176 (3), 417–429.
- Stone, P., Richards, P.C., Kimbell, G.S., Esser, R.P., Reeves, D., 2008. Cretaceous dykes discovered in the Falkland Islands: implications for regional tectonics in the South Atlantic. *J. Geol. Soc. London* 165 (1), 1–4. <https://doi.org/10.1144/0016-76492007-072>.
- Stone, P., 2016. Geology reviewed for the Falkland Islands and their offshore sedimentary basins, South Atlantic Ocean. *Earth Environ. Sci. Trans. R. Soc. Edinb.* 106, 115–143. <https://doi.org/10.1017/S1755691016000049>.
- Stone, P., Kimbell, G.S., Richards, P.C., 2009. Rotation of the Falklands microplate reassessed after recognition of discrete Jurassic and Cretaceous dyke swarms. *Pet. Geosci.* 15 (3), 279–287. <https://doi.org/10.1144/1354-079309-847>.
- Storey, Bryan C., 1995. The role of mantle plumes in continental breakup: case histories from Gondwanaland. *Nature* 377 (6547), 301–308.
- Storey, B.C., Curtis, M.L., Ferris, J.K., Hunter, M.A., Livermore, R.A., 1999. Reconstruction and break-out model for the Falkland Islands within Gondwana. *J. African Earth Sci.* 29 (1), 153–163.
- Thistlewood, L., Leat, P.T., Millar, I.L., Storey, B.C., Vaughan, A.P.M., 1997. Basement geology and Palaeozoic-Mesozoic mafic dykes from the Cape Meredith complex, Falkland Islands: a record of repeated intracontinental extension. *Geol. Mag.* 134 (3), 355–367. <https://doi.org/10.1017/S0016756897007085>.
- Thomas, R.J., Jacobs, J., Eglinton, B.M., 2000. Geochemistry and isotopic evolution of the Mesoproterozoic Cape Meredith Complex, West Falkland. *Geol. Mag.* 137 (5), 537–553. <https://doi.org/10.1017/S0016756800004519>.
- Thomas, R.J., Jacobs, J., Weber, K., 1997. Geology of the Mesoproterozoic Cape Meredith Complex, West Falkland. *The Antarctica Region, Geological Evolution and Processes*, pp. 21–30.
- Thompson, R.W., 1977. Mesozoic Sedimentation on the Eastern Falkland Plateau. *Initial Reports of the Deep Sea Drilling Project* 36, (36). <https://doi.org/10.2973/dsdp.proc.36.122.1977.877891>.
- Thomson, K., 1998. When did the Falklands rotate? *Mar. Pet. Geol.* 15 (8), 723–736. [https://doi.org/10.1016/S0264-8172\(98\)00050-6](https://doi.org/10.1016/S0264-8172(98)00050-6).
- Trewin, N.H., Macdonald, D.I.M., Thomas, C.G.C., 2002. Stratigraphy and sedimentology of the Permian of the Falkland Islands; lithostratigraphic and palaeoenvironmental links with South Africa. *J. Geol. Soc. London* 159 (1), 5–19. <https://doi.org/10.1144/0016-764900-089>.
- Uliana, M.A., Biddle, K., Cerdán, J., 1989. Mesozoic extension and the formation of Argentina sedimentary basins. *Extensional tectonics and stratigraphy of the North Atlantic Margin*, AAPG Mem. 46 (3), 599–613.
- Verduzco, B., Fairhead, J.D., Green, C.M., MacKenzie, C., 2004. New insights into magnetic derivatives for structural mapping. *Lead. Edge* 23 (2), 116–119.
- von Gosen, W., Loske, W., 2004. Tectonic history of the Calcatapul Formation, Chubut province, Argentina, and the “Gastre fault system”. *J. S. Am. Earth Sci.* 18 (1), 73–88. <https://doi.org/10.1016/j.jsames.2004.08.007>.
- Vorster, C., Kramers, J., Beukes, N., van Niekerk, H., 2016. Detrital zircon U-Pb ages of the Palaeozoic Natal Group and Msikaba Formation, Kwazulu-Natal, South Africa: Provenance areas in context of Gondwana. *Geol. Mag.* 153 (3), 460–486. <https://doi.org/10.1017/S0016756815000370>.
- Withjack, M., Jamison, W.R., 1986. Deformation produced by oblique rifting. *Tectonophysics* 126, 99–124.